Extended Essay in Geography

The Classification of Dulwich College Singapore's Microclimate: An Inquiry into the Institution's Degree of Urban and Nature Reserve Microclimatic Character

Research Question: To what extent does Dulwich College Singapore possess an urban or nature reserve microclimate?

Word Count: 3977
Session: May 2021
MLA8

Table of Contents

Acronyms

Urban Heat Island	**UHI**
Dulwich College Singapore	**DCSG**
Sungei Buloh Wetland Reserve	**SBWR**
Jurong East	**JE**
Relative Humidity Percentage	**RH%**
Coronavirus Disease 2019	**COVID-19**

1. Introduction

1.1.Contextualizing the Issue

Urban areas immoderately fall victim to "drought and heatwaves" (Parry et al. 370), resultant of climate change. August 2019's Japanese heatwave saw "57 deaths" and "18,000 hospitalized" (The Japan Times), predominantly in Kyoto (Yajima 1) and Saitama (Yamato et al. 4), cities known for Urban Heat Islands (UHIs). Contextually momentous in the Asian city-state **Singapore**, as 100% of the population live in urban areas (World Bank) and studies from Hien, Roth and Chow suggesting a UHI exists. UHI is an "[urban] area which is warmer than it's surrounding areas" (Metlink). The government has attempted to mitigate UHI and reduce prospective heatwave threats by adapting nature for urban environments (National Parks, *MEDIA FACTSHEET D, Nature Parks as Buffer Parks*). However, recently, since "85%" of the population live in "housing development board homes (HDBs)" (Balázs et al.), studies like Balázs' have begun on "**the distinctive climate of small-scale areas**" (Met Office), or **microclimates**, to see if inhabitants of "high-rise residential buildings" (Balázs et al.) are in danger of local resultant climatic processes. Likewise, classifying Dulwich College Singapore's (DCSG) microclimate will be seminal in protecting its community from potential dangers (localized heatwaves). This paper may contribute to the larger study of microclimates in biophilic-designed buildings.

1.2. Investigative Approach

The investigation compares meteorological data (temperature, relative humidity, wind speed, light intensity) of DCSG and two other microclimates in western Singapore, collected by the candidate over 4 days in July. It uses secondary sources to lay theoretical foundations and support choice of sites.

Aim: To determine if DCSG's microclimate is more like Jurong East (JE), a secondary central business district (CBD) with an urban microclimate, or Sungei Buloh Wetland Reserve (SBWR), a nature reserve microclimate.

Research question: 'To what extent does Dulwich College Singapore possess an urban or nature reserve microclimate?'.

The research question is adequate as it investigates the degree of microclimate, rather than finding a definitive microclimate.

1.3. Spatial and Climatic Context

July falls under the Southwest monsoon in Singapore (Meteorological Service Singapore).

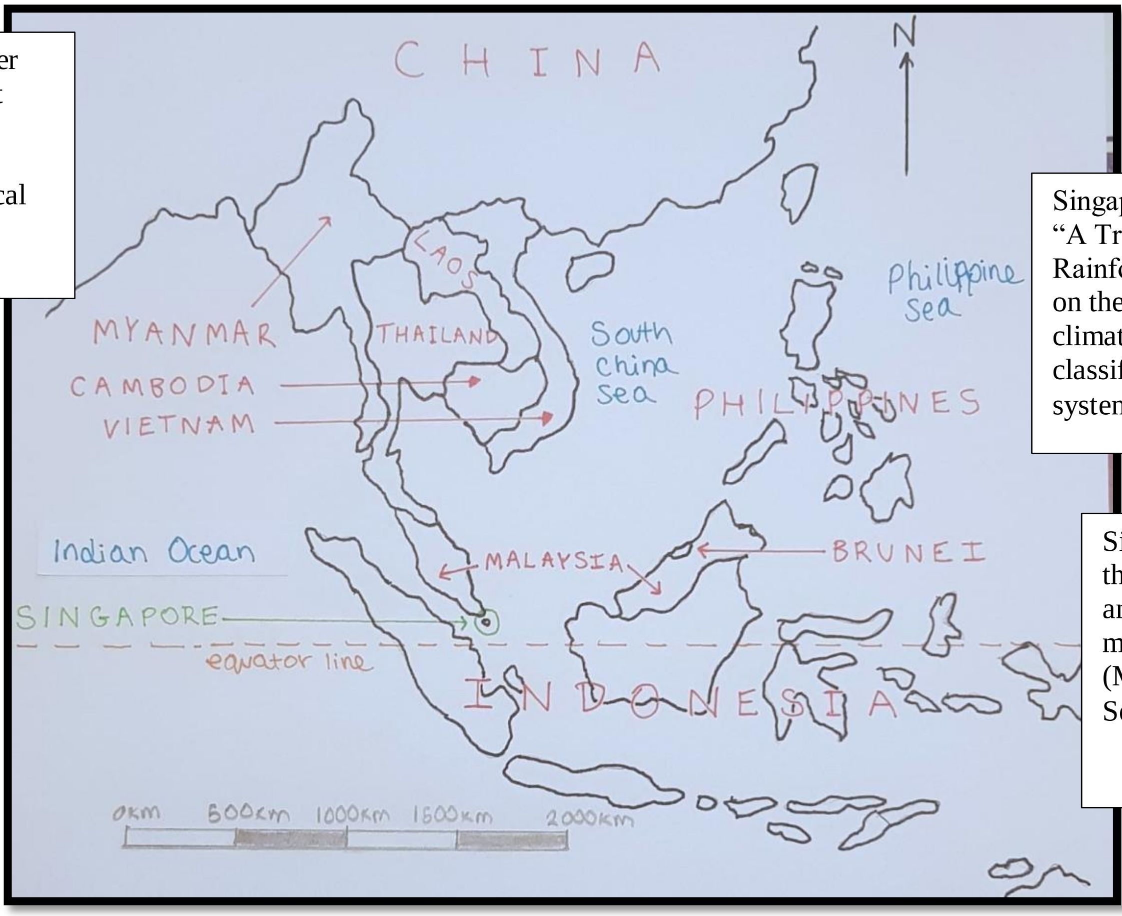

Singapore is "Af" or "A Tropical Rainforest Climate" on the Köppen climate classification system. (Li et al.)

Singapore goes through 2 monsoon and 2 inter-monsoon periods, (Meteorological Service Singapore).

Figure 1 - Hand drawn map of South East Asia by the candidate, based on the work of Morgan and Staples

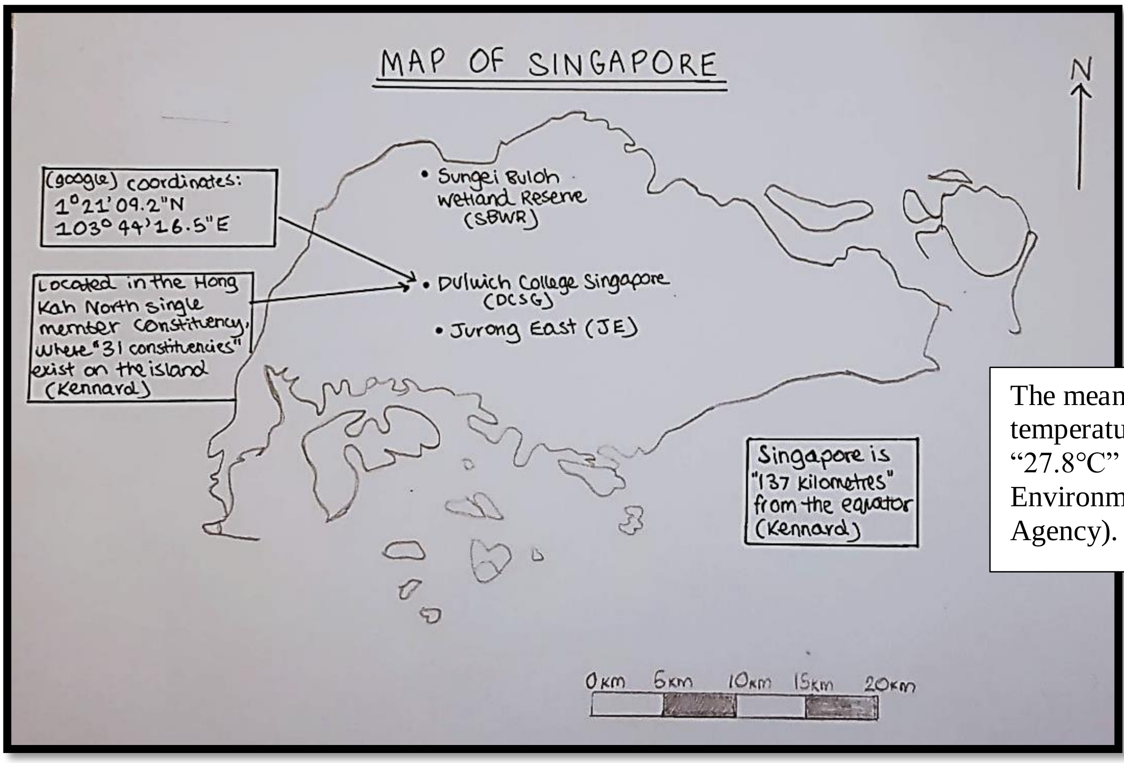

The mean temperature of July is "27.8°C" (National Environment Agency).

Figure 2 - Hand drawn map of Singapore by the candidate, based on the work of Koninck

Singapore lacks reliance on the primary CBD as urban morphology arose from urban realms generation (fig.5), categorized by "economic functions" (Godfrey 580). Spatial distribution (fig.4) suggests widespread anthropogenic activity.

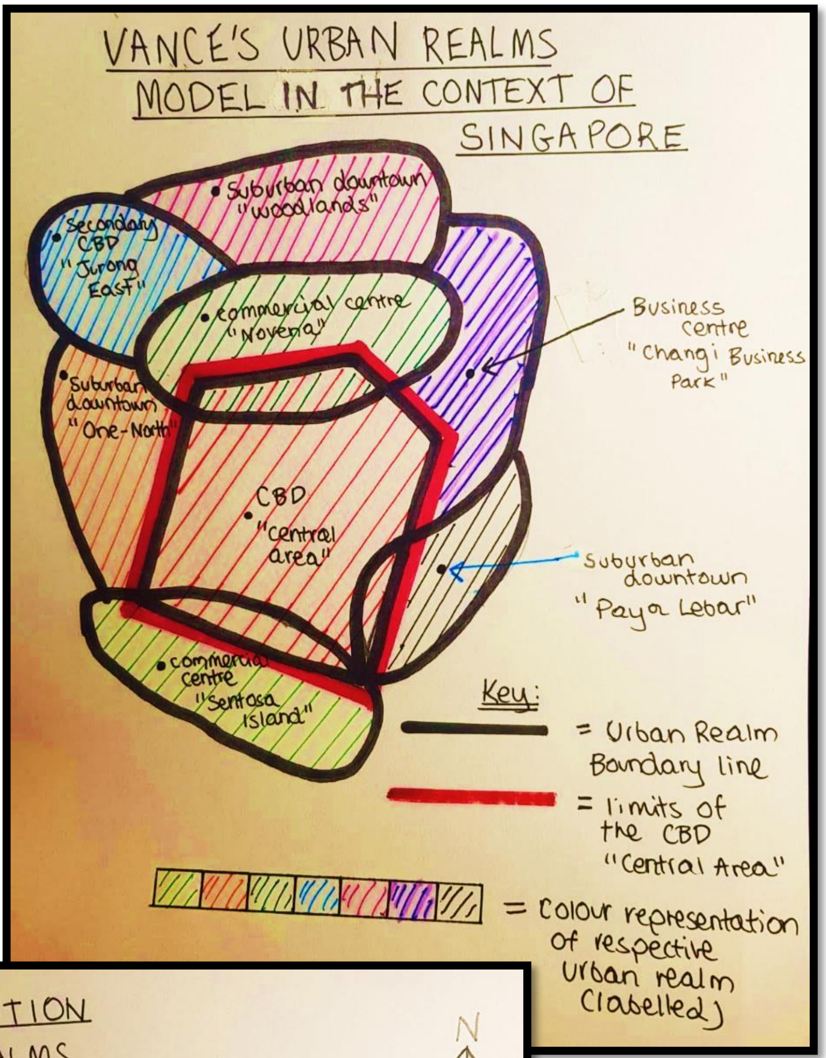

Figure 3 - Hand drawn map of Vance's Urban Realms Model in the context of Singapore by the candidate, based on the work of Albahae with label ideas from URA, Xiu and Vincent

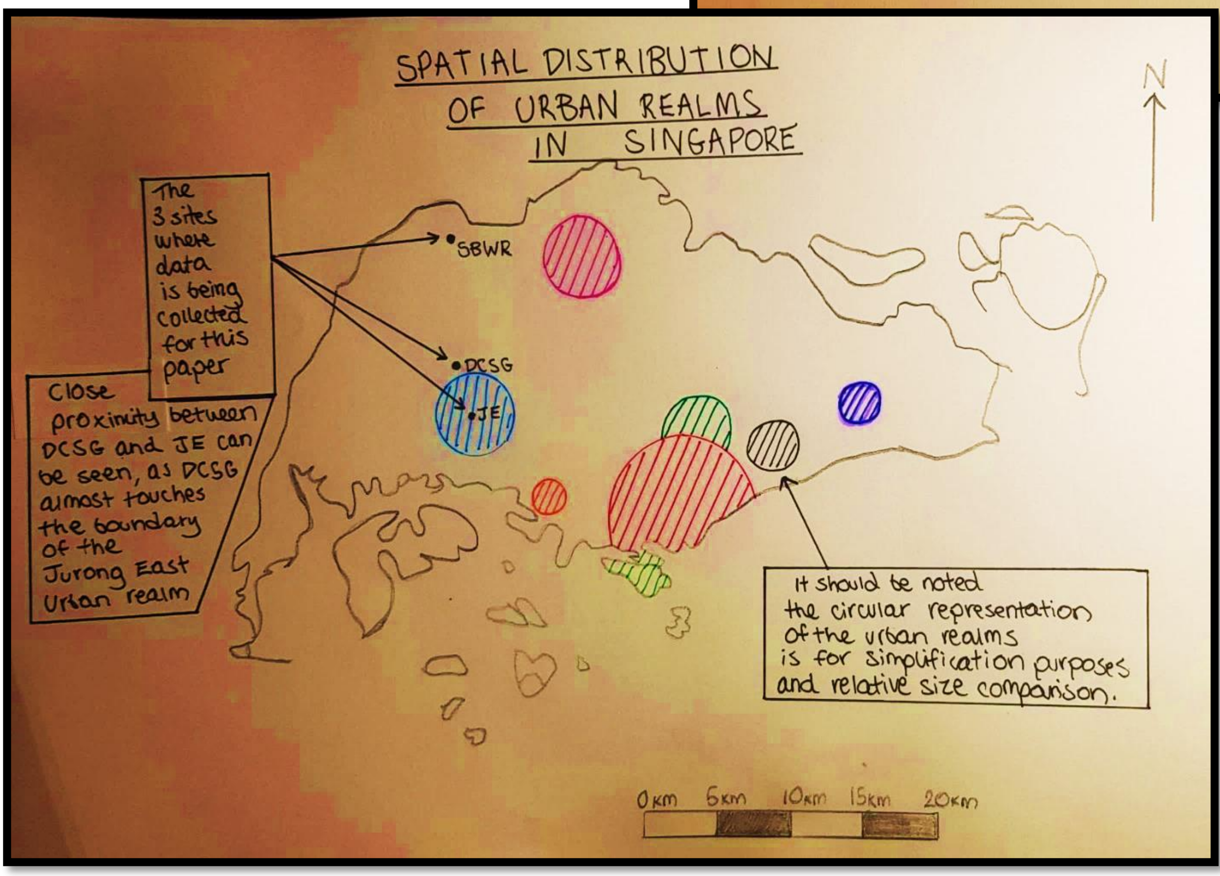

Figure 4 - Hand drawn map of Singapore by candidate, illustrating the spatial distribution of urban realms from figure 3, based on the work of Koninck

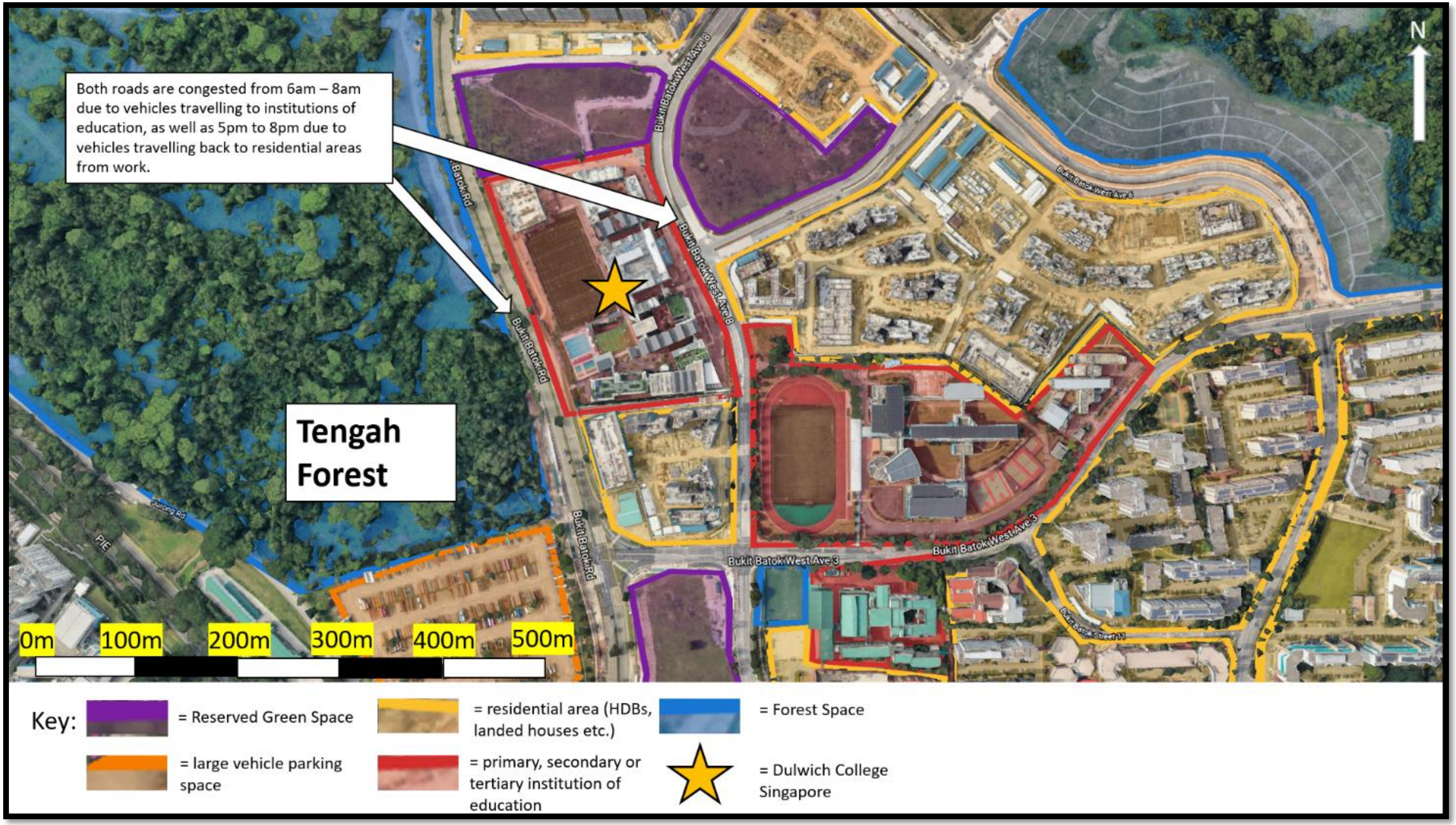

Figure 5 - Map of part of Hong Kah North (constituency - North of Jurong East), illustrating DCSG in relation to other land uses, adapted from Google Earth

DCSG's spatial situation disallows microclimate classification straightforwardly; it has a biophilic design (structure embeds greenery) and is adjacent to a forest. However, Anthropogenic heat is created on-site and on nearby roads. It is proximal to JE (secondary CBD) and urbanized residential/institutional land (fig.5).

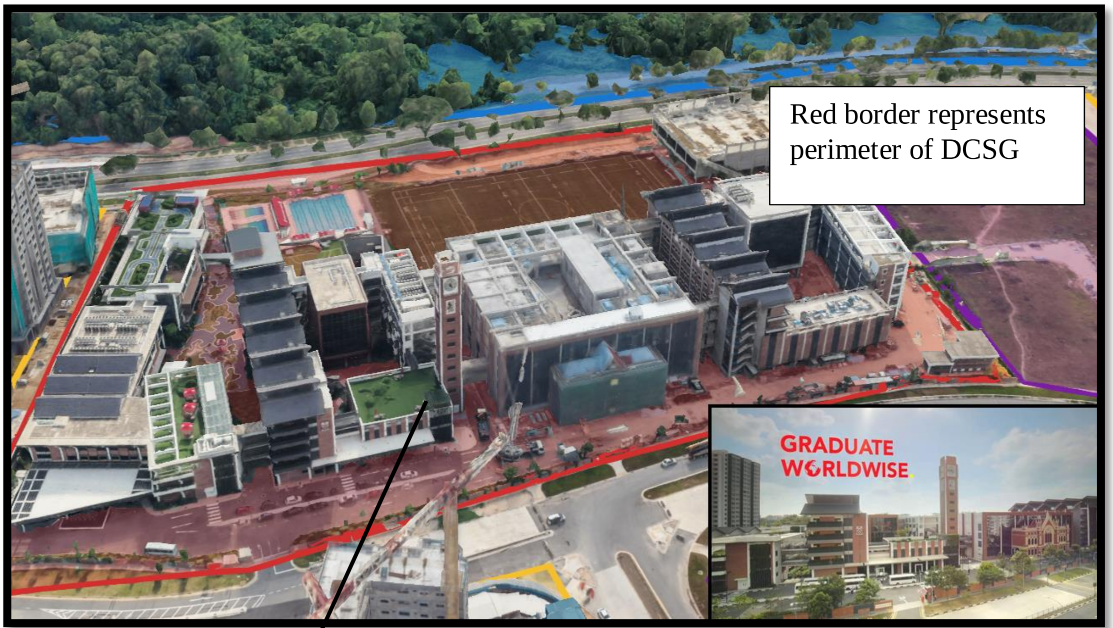

Figure 6 - 3D view of DCSG (Google Earth) during construction, post-construction picture in the bottom right (Dulwich College Singapore)

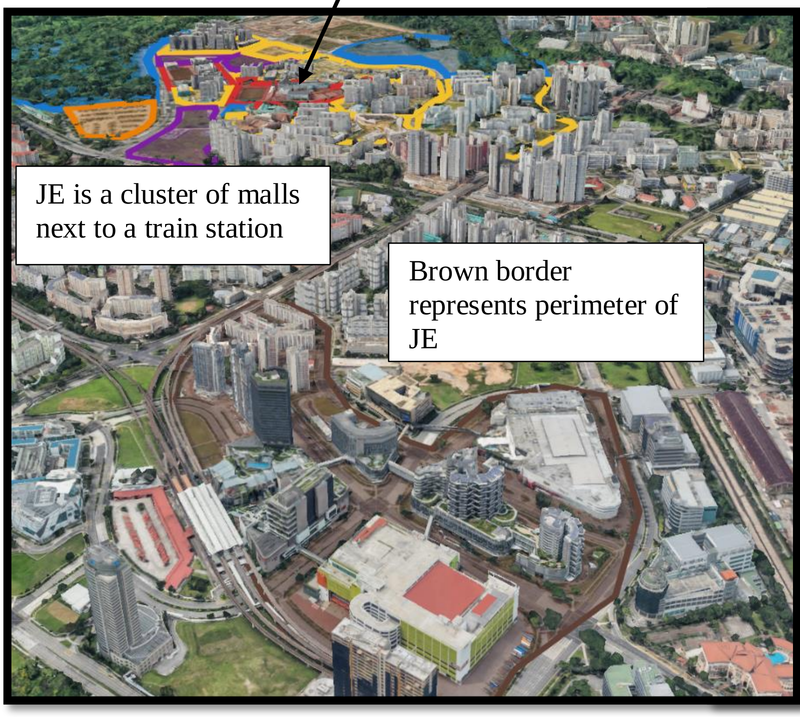

Figure 7 – 3D aerial view of JE (Google Earth)

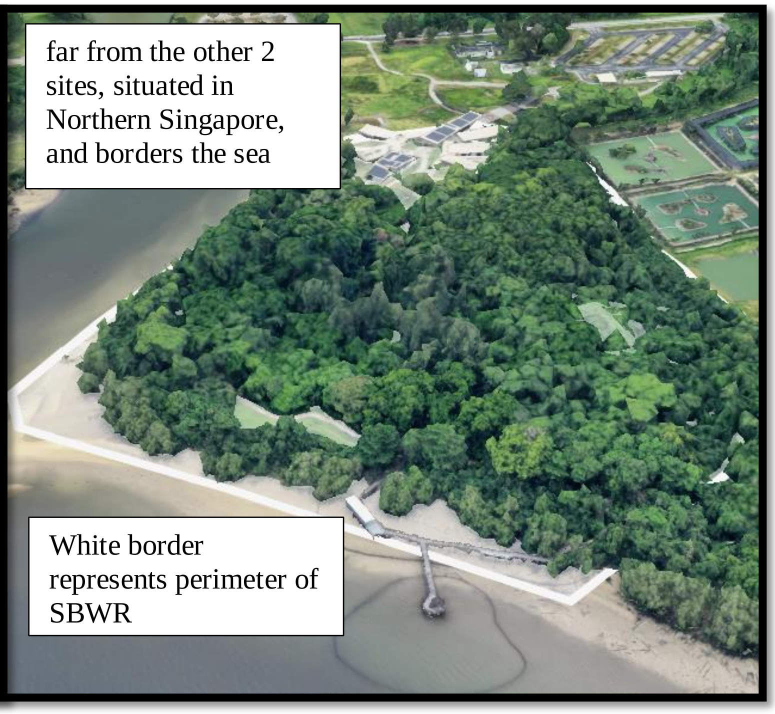

Figure 8 – 3D aerial view of SBWR (Google Earth)

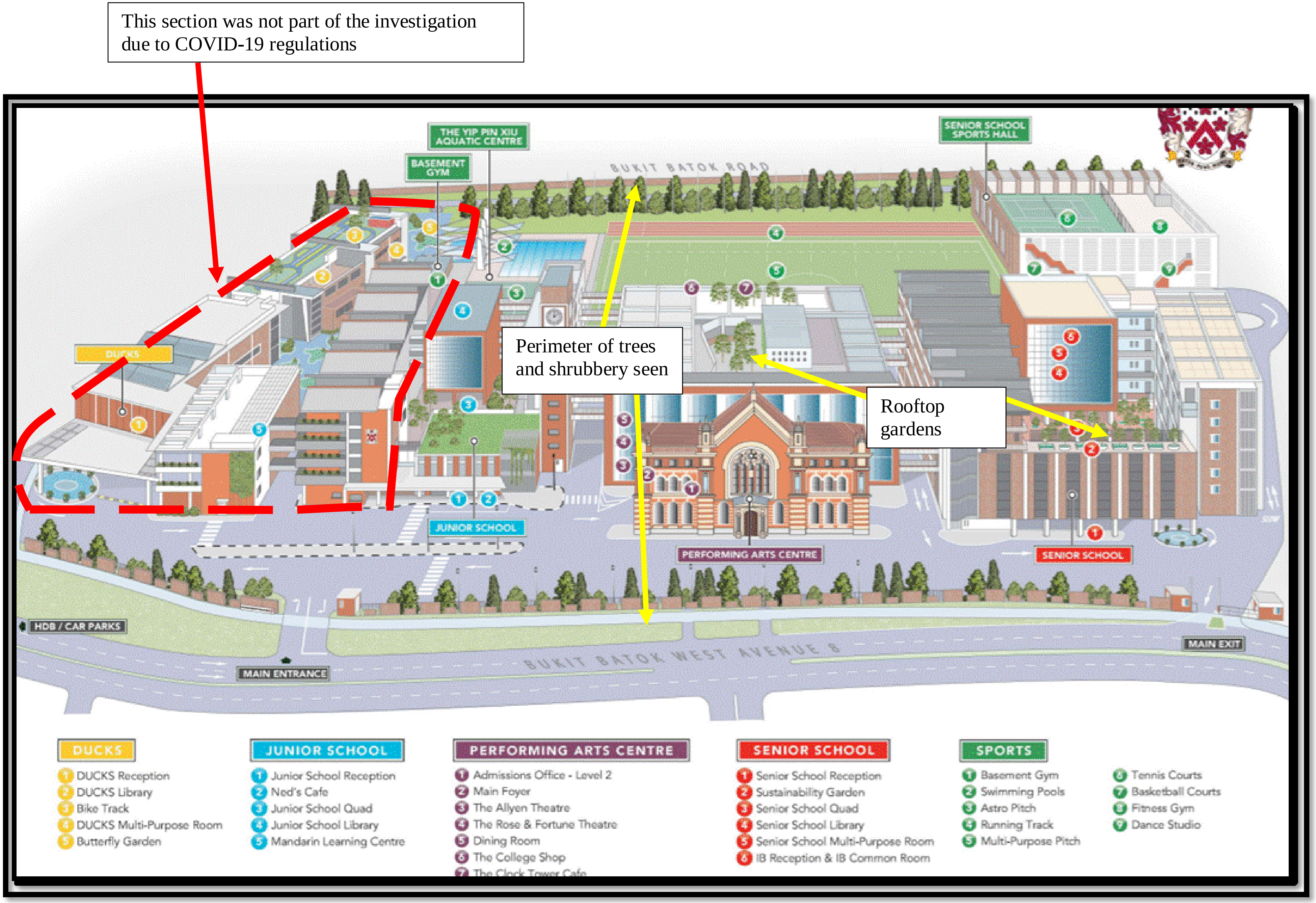

Figure 9 - Map produced for visitors of DCSG, adapted from (Dulwich College Singapore)

1.4. Limitations

Comparisons are less accurate as data is not collected on the same day/time (avoiding prolonged environmental exposure). Consequential, as studies place emphasis on temporal data. Expected anthropogenic processes are lessened due to COVID-19.

2. Microclimate Background

2.1. Urban Microclimates

2.1.1. Urban Microclimate Theory

Burdett and Urban Hub synonymously use 'UHI' and 'Urban Microclimate' in their blogs, contradicting Nagle and Cooke's textbook description distinguishing phenomena; literature by well-versed geographical scholars implies greater credibility. Aforementioned sources fail to geographically contextualise urban microclimates. Wong et al.'s Singapore-focused, peer-reviewed, 2018 journal article makes a distinction supporting the textbook. Hence, Nagle and Cooke and Wong et al.'s work provide theoretical basis.

Feature of Urban Area	Resultant Processes	Urban Microclimate Feature
1. High proportion of "hygroscopic particles" (Nagle and Cooke)	Lower proportions of water vapour in the air, thereby less moisture to hold, leading to lower relative humidity (RH%). These particles can also block solar radiation due to heightened cloud formation	Low relative humidity Low light intensity
2. Tall Buildings	Create lower "sky view factor" (SVF) meaning less solar radiation reaching the ground. Tall buildings block air flow, decreasing wind speeds.	Low light intensity Low wind speed

Feature of Urban Area	Resultant Processes	Urban Microclimate Feature
3. Combustive processes (Cars, A.C. Units)	Surfaces retain anthropogenic heat, re-radiated to air, facilitating increased evaporation and cloud formation frequency, causing lower solar radiance to reach the ground.	High temperature Low light intensity
4. Low albedo surfaces	Surfaces have high heat retention (fig.10) which is re-radiated to the air.	High temperature

Table 1 - Features of urban areas, expected resultant processes and related microclimate feature. Contents adapted from Nagle and Cooke, Wong et al.

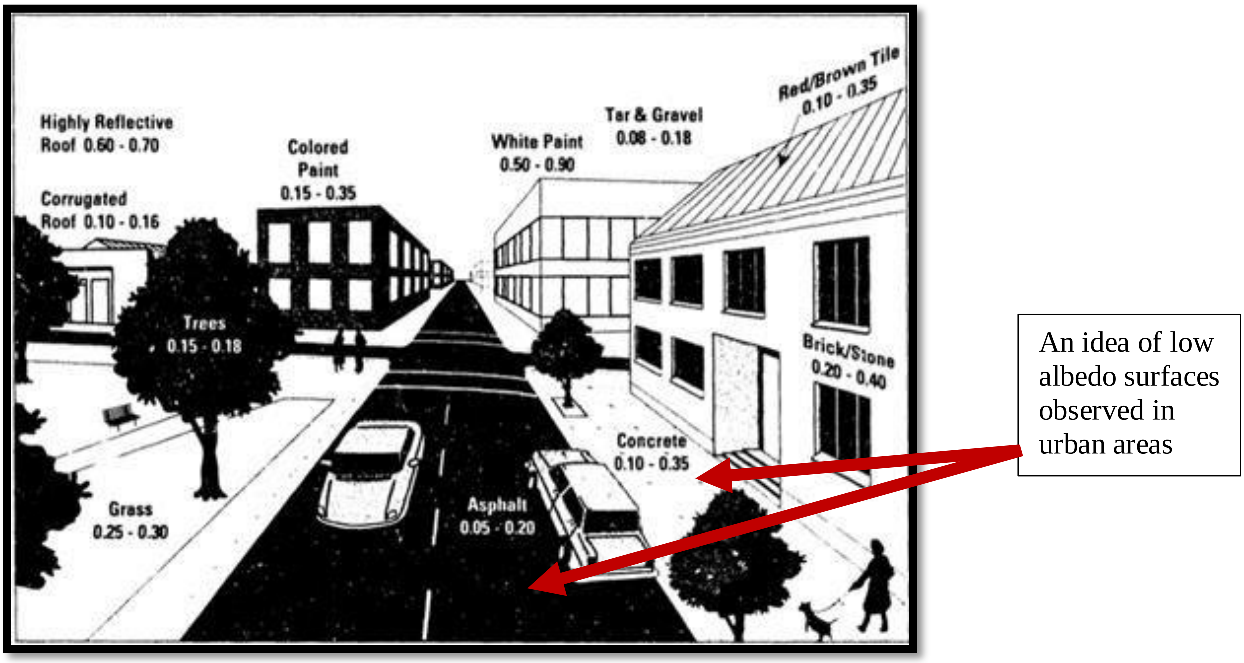

Figure 10 –Albedo of surfaces in a city context (Jacobs and Delaney, Adapting to urban heat in Penrith)

2.1.2. Classifying Jurong East

Secondary sources identify a comparable urban microclimate to DCSG, Roth and T.L.Chow suggest "secondary UHI peaks in Jurong Industrial Estate". Although UHI validates the temperature aspect, it fails to holistically categorize a site through other factors. Wong et al.'s aforementioned study investigated JE, their results are below.

p = 0.05, indicates statistically significant results and did not take place by chance.

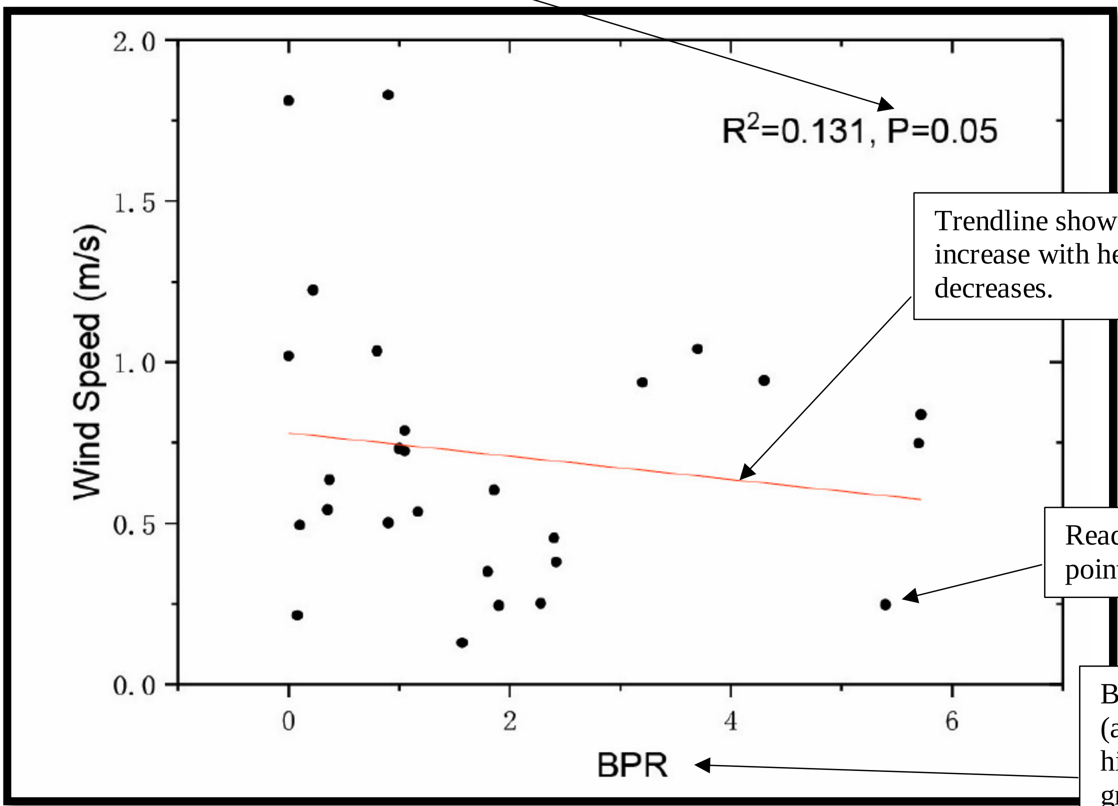

Trendline shows as buildings increase with height, wind speed decreases.

Readings at data points during daytime

Building plot ratio (arbitrary units) – higher ratio implies greater built-up floor area/ floors on the building.

Figure 11 – Wind speeds (m/s) relationship with Building Plot Ratio in JE (Wong et al.) in a scatterplot

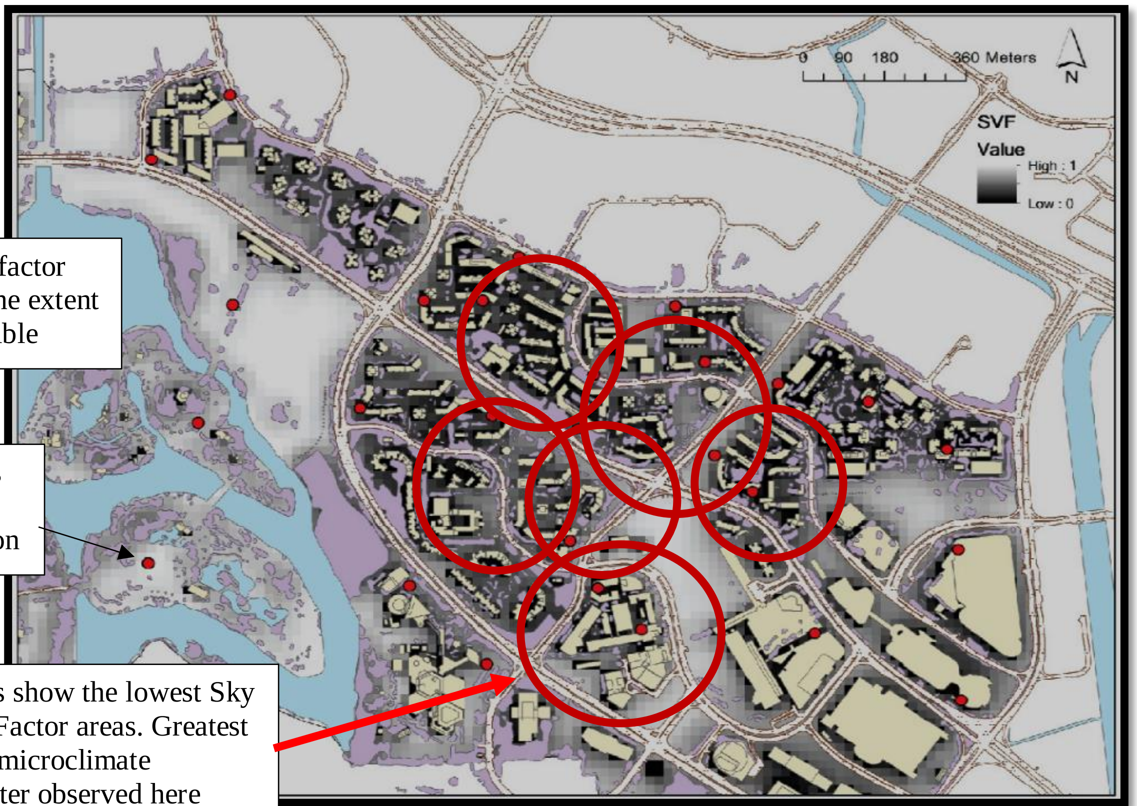

Sky view factor refers to the extent of sky visible

Data points of the investigation

Circles show the lowest Sky View Factor areas. Greatest urban microclimate character observed here

Figure 12 – Spatial Distribution of 'Sky View Factor' (SVF) in JE (Wong et al.)

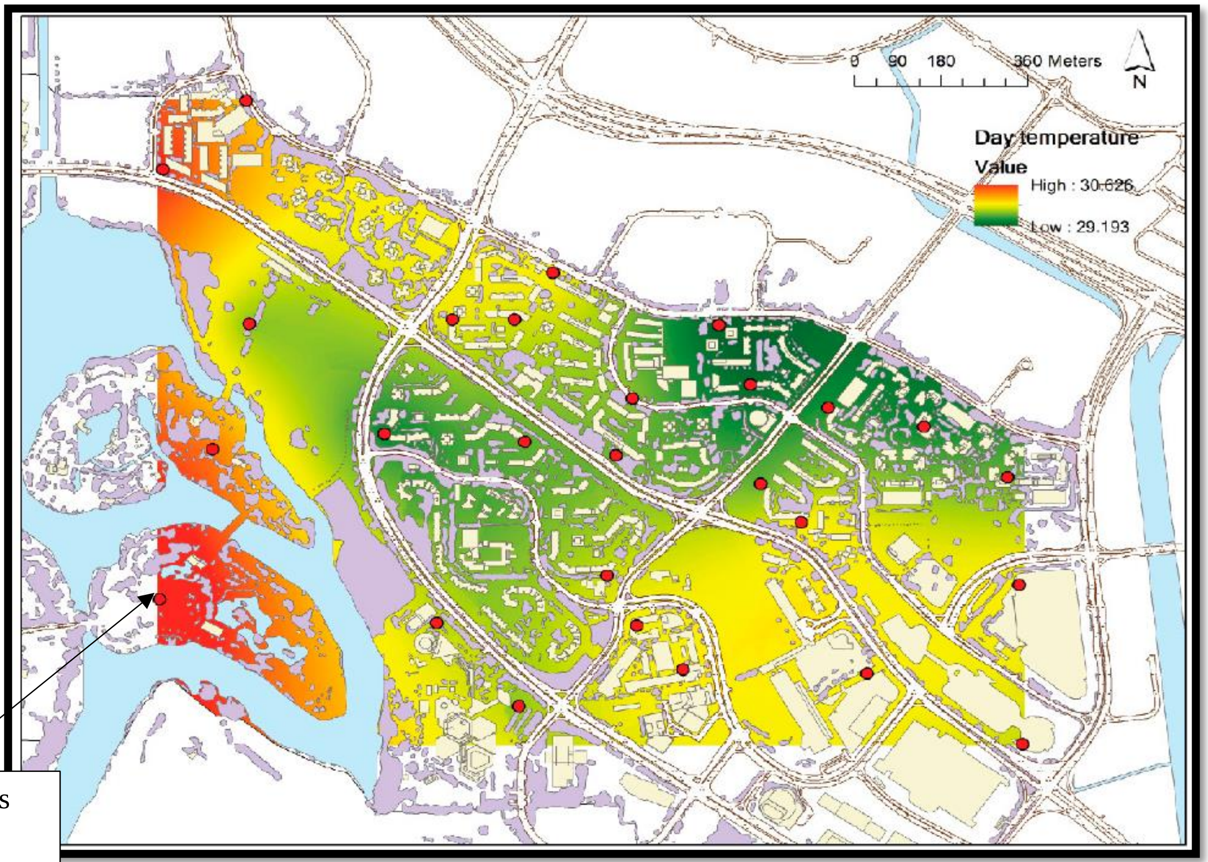

Data points of the investigation

Figure 13 – Heat map of temperature (℃) during the day at JE (Wong et al.)

Figures 13 and 14 show a broad spectrum of temperatures.

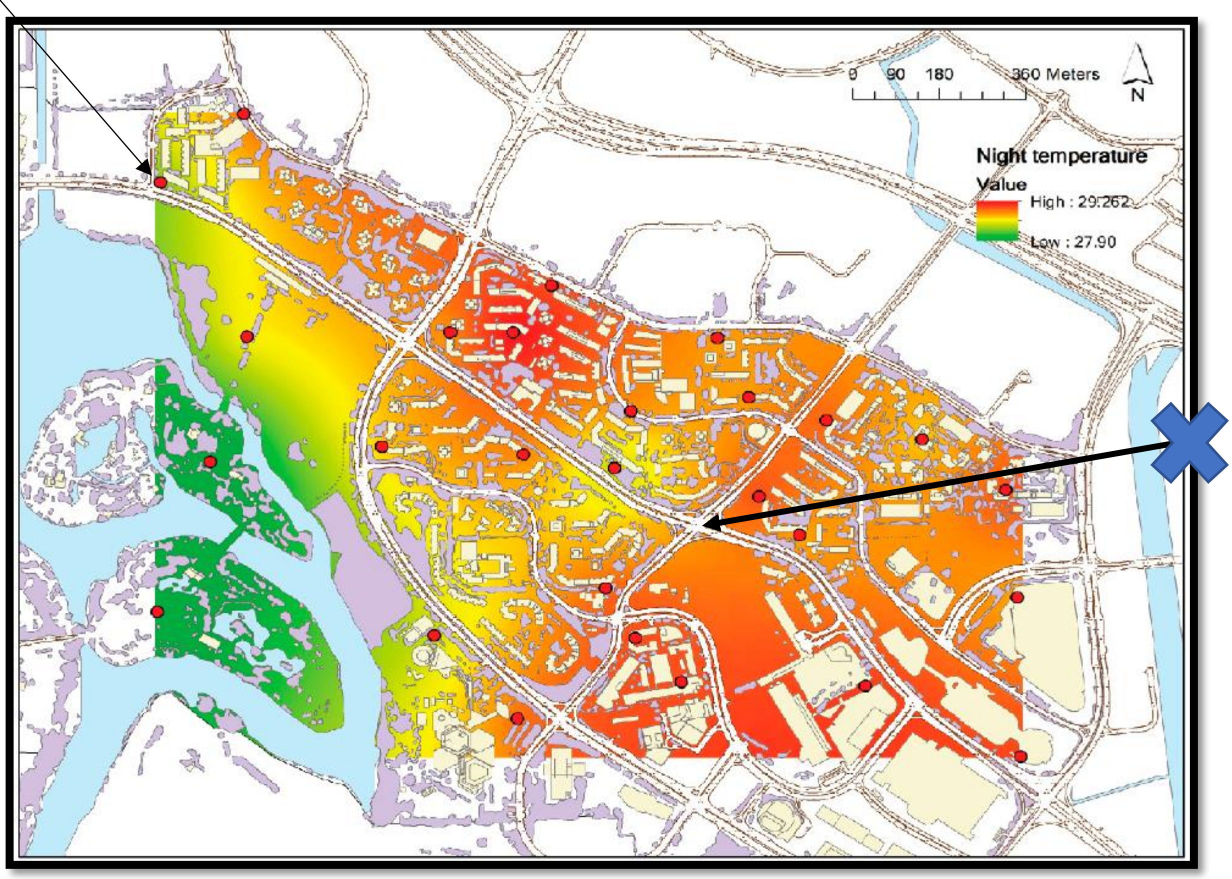

Figure 14 – Heat map of temperature (℃) during the night at JE (Wong et al.)

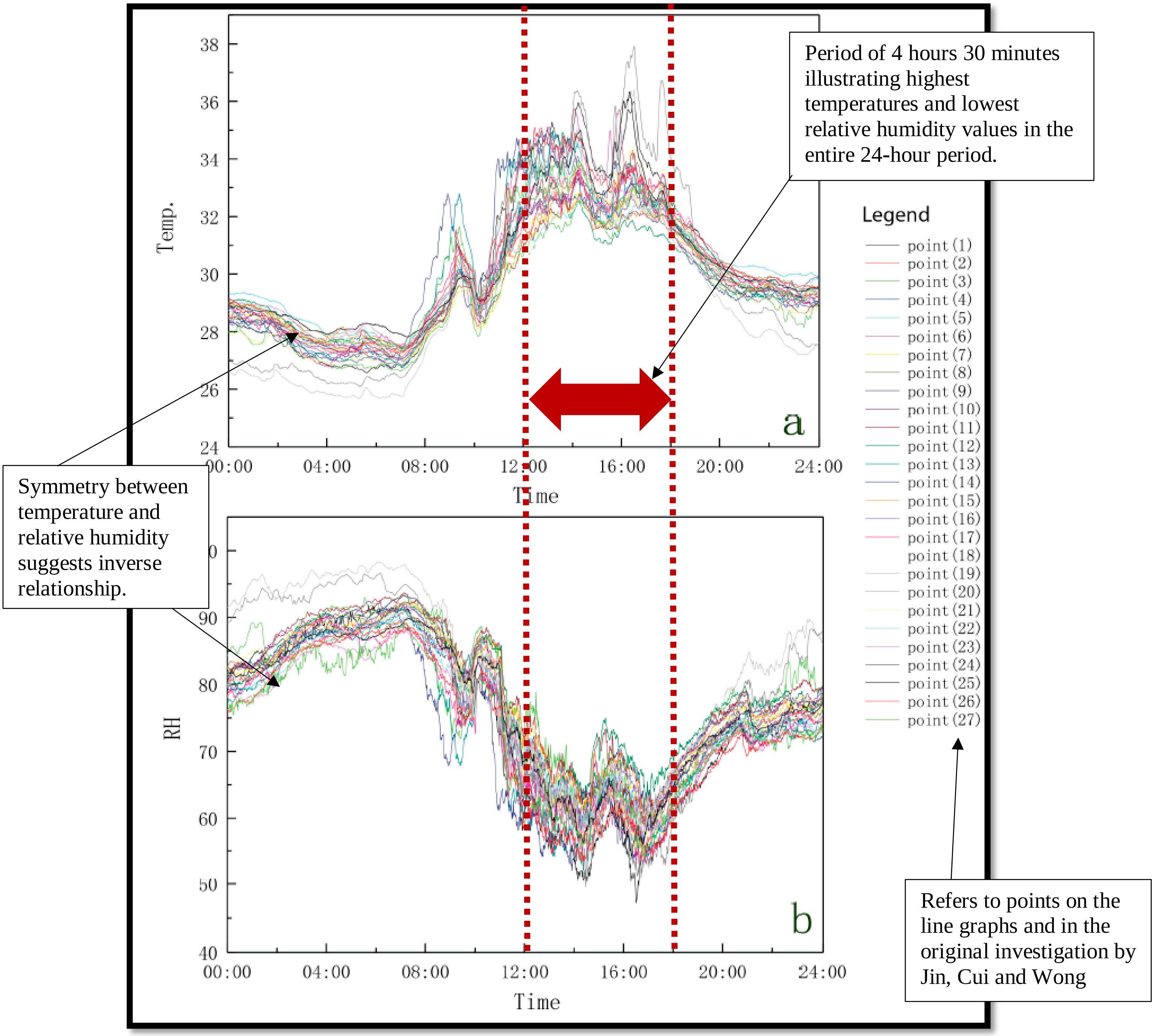

Figure 15 – Compound line graphs for Temperature (℃) (Temp.) (a) and Relative humidity (%) (RH) (b) over a 24 hour period in JE (Wong et al.)

Wong's data patterns in accordance with urban microclimate features exhorts **JE's suitability as an urban microclimate for comparison with DCSG**, additionally underscoring the temporal nature of microclimates. Figs.13 and 14 illustrate disparate sets of temperature distinguished temporally, attributing an urban microclimate to night-time. However, Fig. 8 renounces this with greater specificity, categorizing the greatest urban microclimate presence to 12:00-16:00 through temperature and relative humidity. Fig.14's blue cross marks JE's urban microclimatic nexus, where data transects for this investigation will propagate.

2.2. Nature Reserve Microclimates

Figure 16 – Collage of photographs at DCSG (Candidate)

Figure 17 – Collage of photographs at SBWR (Candidate)

Like DCSG, nature reserves contain plentiful vegetation whilst maintaining accessibility. Met Office suggests forest microclimates’ distinctive features are based upon type and volume of vegetation, it is possible DCSG and SBWR share a microclimate due to shared fauna (figs.16,17).

SBWR’s nature reserve microclimate, one of 4 in Singapore, did not have accessible sources detailing features and processes, hence sources for similar microclimates were explored. Naim et al.’s contemporary (2012) and geographically relevant (Malaysian) results on rainforest microclimates illustrate differences between a built up and interior forest site for meteorological variables (Fig.18). Nature reserves are based off existing rainforests, hence using rainforest-based sources do not largely hinder theory. Results act as a springboard to draw out relevant theories, it is not taken at face value as context of nature reserve site is necessary (table 2).

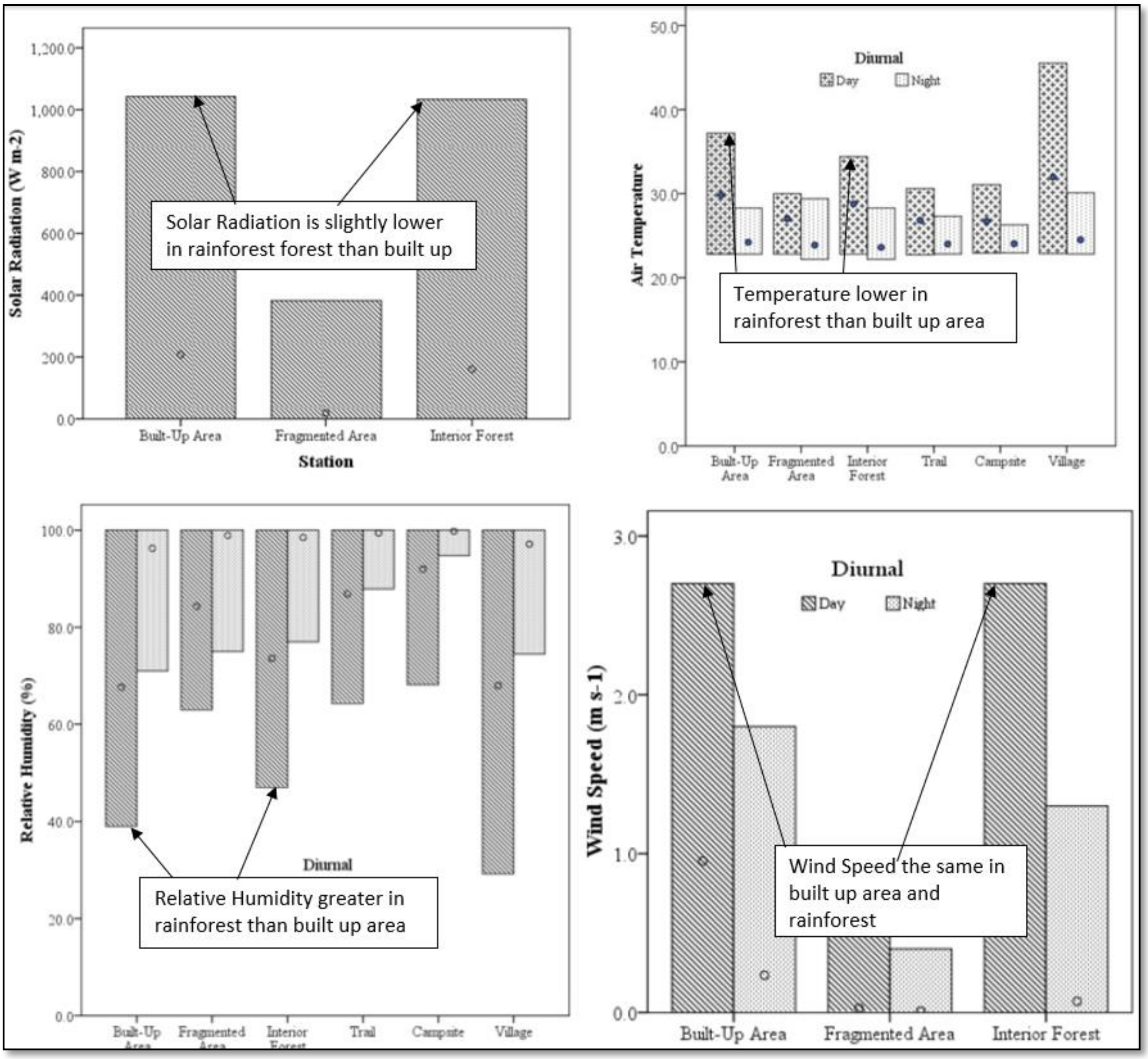

Figure 18 - Graphs of Solar Radiation, Relative Humidity, Wind Speed and Air Temperature Adapted from Naim et al.

Feature of Nature Reserve	Resultant Processes	Nature Reserve Microclimate Feature
Abundance of vegetation	Heightened local evapotranspiration cycle due to vegetation abundance; owing to moisture available and low temperatures, relative humidity is high.	High relative humidity

Feature of Nature Reserve	Resultant Processes	Nature Reserve Microclimate Feature
Flexible structure	Wind passes through nature reserves easily due to lack of resistive material (i.e., buildings), flexible vegetation permits high wind speeds.	High wind speed
Low anthropogenic activity (combustion, human/animal activity)	frequent winds cause cooling, low anthropogenic heat created.	Low temperature
Partially forested	Solar radiation can reach the ground in non-forested parts.	High light intensity

Table 2 - Features of Nature Reserves, expected resultant processes and related microclimate feature. Contents adapted from Nagle and Cooke & Met Office

3. Hypotheses

DCSG could be climatically influenced by Tengah forest and surrounding green spaces and share a similar vegetation structure to SBWR. However, spatial exploration highlights clustering of tall buildings in DCSG, leading to low wind speeds and light intensity due to wind resistance and scattering of short-wave solar radiation respectively (Nagle and Cooke). Like JE's malls, DCSG generates masses of heat for air conditioning; peripherally, the surfaces and albedo values are similar and hence high temperatures. Hygroscopic particles and anthropogenic heat produced by vehicles on roads outside DCSG lead to low light intensity and humidity. Therefore, the hypotheses support the urban over nature reserve microclimate. As qualitative data was not the primary method of data collection, emphasis is placed on numeracy.

H_1: Temperature at DCSG is more numerically like JE than SBWR

H_2: RH% at DCSG is more numerically like JE than SBWR

H_3: Light intensity at DCSG is more numerically like JE than SBWR

H_4: Wind speed at DCSG is more numerically like JE than SBWR

4. Literature Review

Microclimate literature, often regionally focused, needed contextual relevance due to climatic variability. To limit bias, international works were read to garner alternative perspectives as Singaporean literature often came from same institutions (NUS). Researchers concluded similar microclimate phenomena pertaining to meteorological factors, underlining new interpretations like multiple urban microclimates contributing to larger UHIs (Wong et al. 2), whilst others argued microclimates homogenize in residential areas (Hall et al. 1). It was found microclimate research conventions allow specificity in classification to a single site (nature reserve microclimate) or type of land (urban microclimate). Singaporean papers primarily collected meteorological data over long periods, diurnally and nocturnally, showing temporal variability in microclimatic character (fig.15). Balázs and Wong's studies collected data using weather stations. Though non-replicable in scale or accuracy, it is adaptable by measuring similar variables using alternative equipment in a local context. Secondary data was not prevalent in Singaporean research, conceivably due to financial barriers the National Environment Agency places on historical meteorological records and necessity of contemporary data to draw accurate microclimatic conclusions. No emphasis was placed on sampling methods or intervals, however, peripherally, a large spatial distribution of data points was achieved in most studies. Data driven by software simulation was unpopular, as some researchers suggested "microclimate [simulation] models vary widely based on physical basis" (Balázas et al. 4). Researchers' choice of spatial exploration used Google Maps/Earth for accessibility, it was found Geographic Information Systems often incurred costs and were cumulatively poor on modelling Singapore (i.e. ARCGIS). As information is regularly updated and intends to educate people on geography theory (aside from research papers), textbooks and national meteorological organizations are especially credible. Both works are the conglomeration of multiple persons' understandings, therefore information is likely accurate. Potential flaws in literature used include overreliance on researchers, as conclusions may include implicit biases, opposed to textbooks and meteorological sites where it is less likely. This decision was made to achieve a contemporary and local view of microclimates.

5. Data methodology

If repeated, this methodology would not be feasible in sites in different countries or states, as an underlying macroclimate across Singapore is assumed. This methodology is loosely based off Balázs and Wong et al.'s work.

5.1. Preliminary Testing

Preliminary testing at a local park found the multimeter's hygrometer (relative humidity) was malfunctioning. Instead of discarding this variable, a wet-dry bulb was made, in sling-psychrometer style. A relative humidity table until 35°C was not found; therefore, an online calculator was used to calculate values (Appendix A). It was calibrated by being placed in a cup of salt overnight, calculated relative humidity percentage should have read 75% but since 64% was observed, 11% was added to all values.

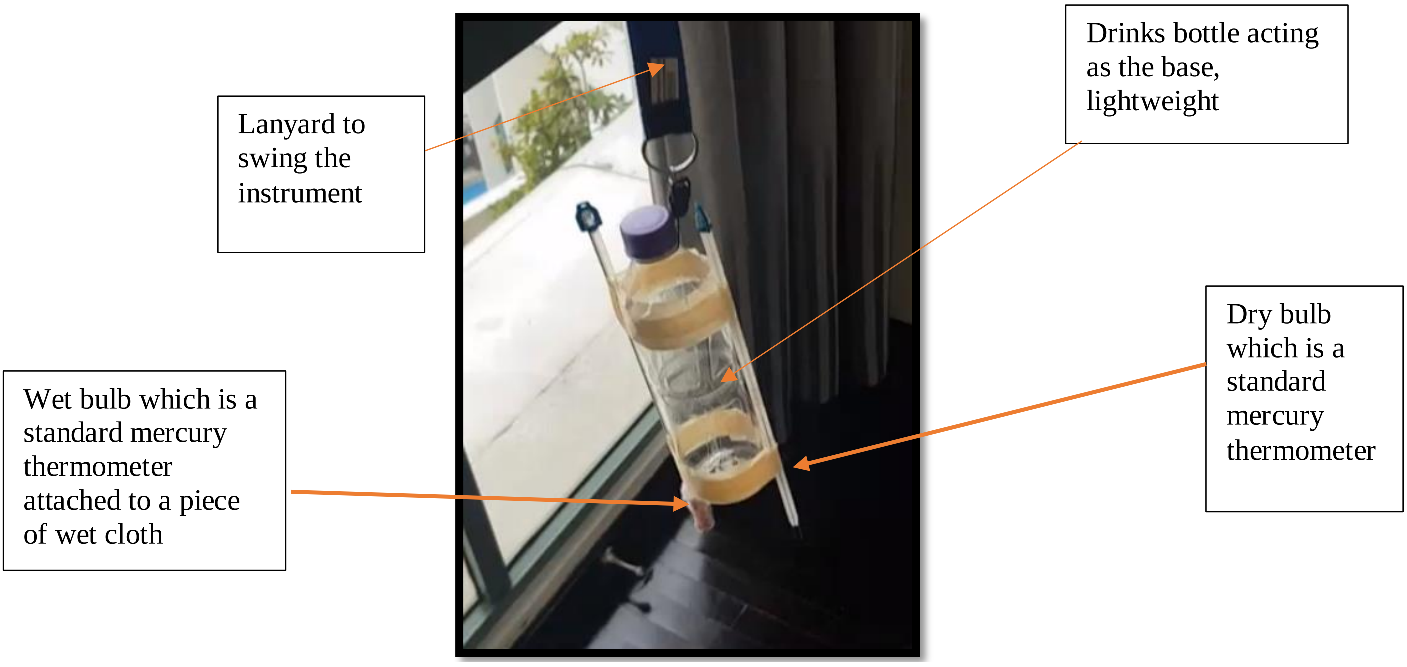

Figure 19 - Homemade wet-dry bulb by Candidate, photograph by candidate

5.2. Risk Assessment

Due to COVID-19, masks will be worn, social-distancing maintained, and areas of known clusters and lengthy exposure to surroundings are avoided. Restricted areas on all 3 sites may be dangerous (construction etc.), maps are therefore followed.

5.3.Apparatus

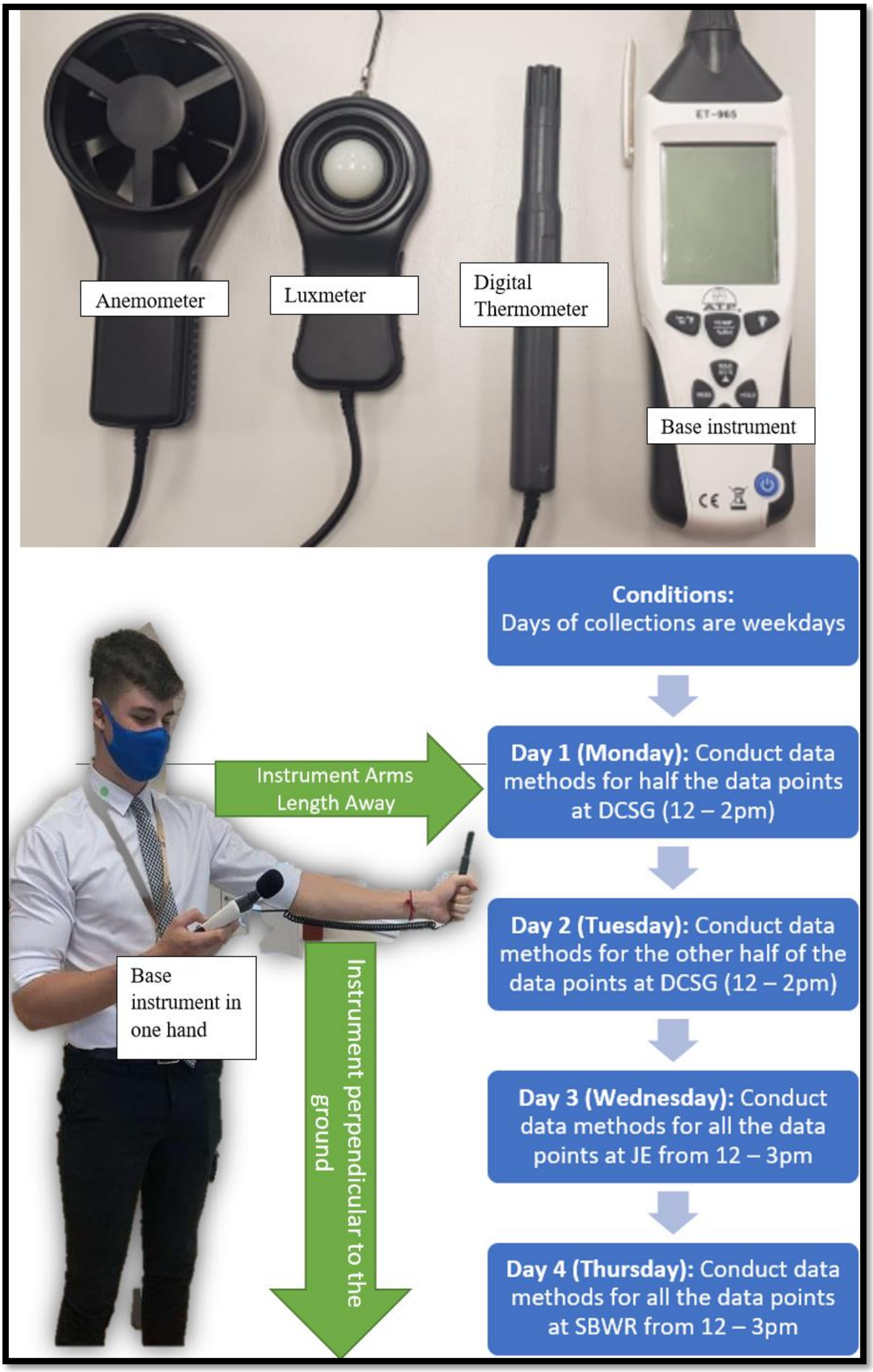

Figure 20 - Photograph of equipment, photograph of how to use the equipment and timeline for data collection, photographs taken by candidate

Piece of Apparatus	**Relevance to hypothesis number**	**Use and measurement justification**
Digital Thermometer (±0.05°C)	1	Measures air temperature. Advantageous due to accuracy and hypersensitive nature as minute differences are observed between sites. Disadvantageous if held too close to a surface (i.e. ground) as temperature changes drastically.
Wet-dry bulb (±0.5%)	2	Measures relative humidity (RH%). Values from wet-dry bulbs were put into an online calculator (Appendix A). Instrument is advantageous as it is not electronically driven, therefore not affected by power loss. However, collecting data takes 2 minutes per point, making it inefficient.
Luxmeter (±0.05 lx)	3	Measures light intensity, highly sensitive allowing for minute differences in data points to be seen.
Anemometer (±0.05m/s)	4	Measures wind speed. Fan-based anemometer was used instead of a cup-based anemometer as it can pick up lower wind speeds easily.
Base instrument	All	All but 1 equipment attaches this instrument to read values. Although accessible in use, the poor battery life may hinder data collection.
Camera, Notebook and Pen	All	To note surroundings and results.
Bottle of water (100ml)	2	To maintain wetness of wet-bulb’s cloth.

Table 3 – Apparatus, respective hypothesis, and justification of use

5.4. Hypotheses methods

At each data point, conduct the cumulative method within an estimated 6-minute window.

5.4.1. Hypothesis 1, 3 & 4 method

Attach the respective apparatus to the base instrument via the port and hold perpendicular to the ground at chest level (fig.20). Press ‘power’ ( ) on the base instrument. Count for 10 seconds and press ‘Max’. To provide the highest value collected in that time. Confirm units are correct by pressing ‘unit’. Note displayed values in the journal.

Luxmeter’s bulb should face upwards. The anemometer’s arrow should face away from the user, so the wind can pass through the correct side.

5.4.2. Hypothesis 2 method

Open the bottle of water and dip the wet bulb’s cloth into it. Wrap wet-dry bulb around wrist and secure. Swing for 30 seconds arm’s length away, making sure others are not around. After, at eye level to avoid parallax, read values for each bulb. Note values down in the journal. At the end of data collection, calculate values for relative humidity using the online calculator.

5.5.Data Transects

Line sampling in a systematic method, so the whole area is covered, however there is a degree of bias as not all spots have an equal chance of being picked.

Coordinates of the 60 data points, 60 chosen as it was realistic in the time frame.

Restricted access point – data was not collected, 59 data points in total

Transect lines and direction

Time and day of each transect

Figure 21 - Transect Map of DCSG, adapted from Landezine

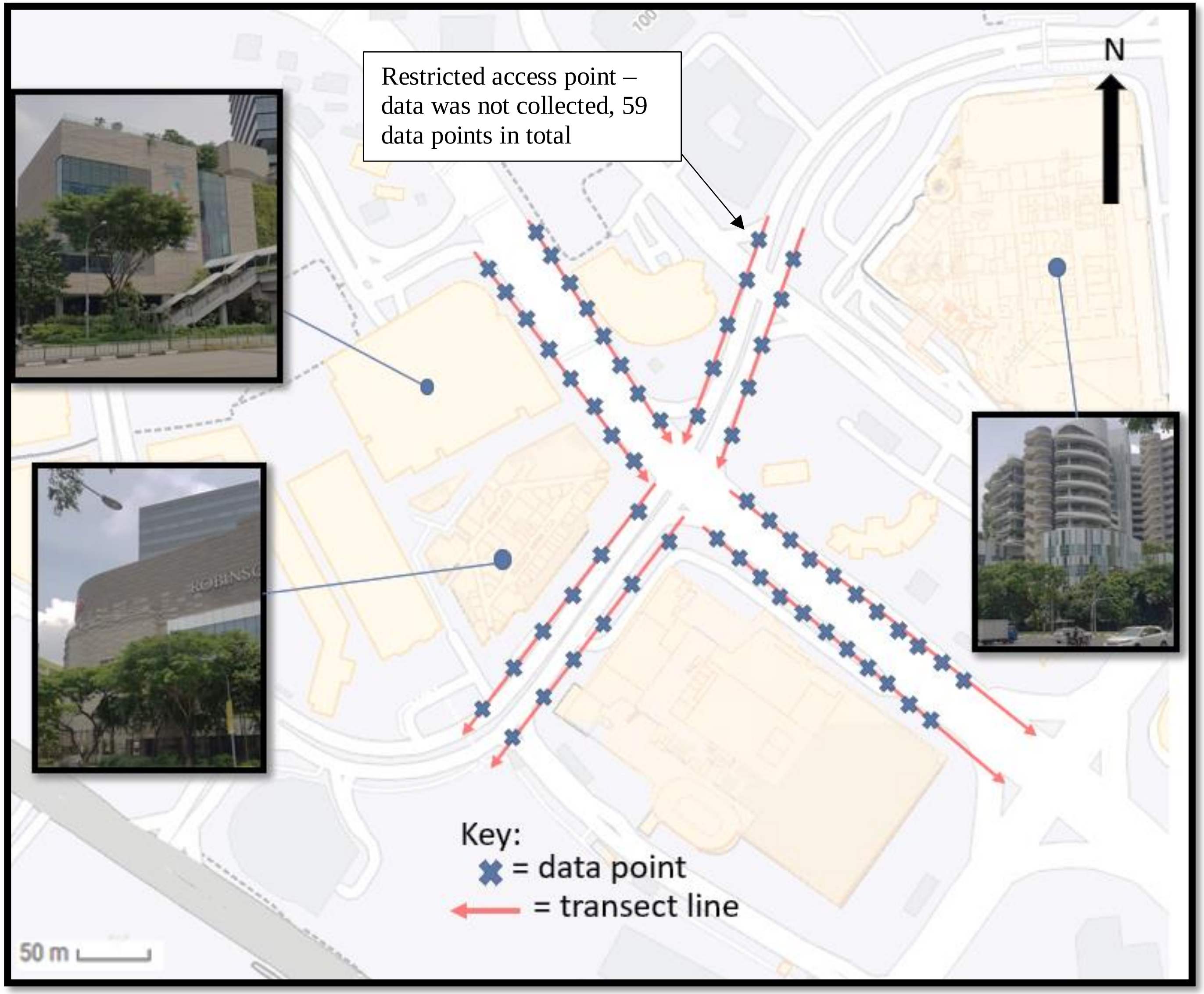

Figure 22 - Transect map of JE, adapted from GoogleMyMaps, pictures by candidate

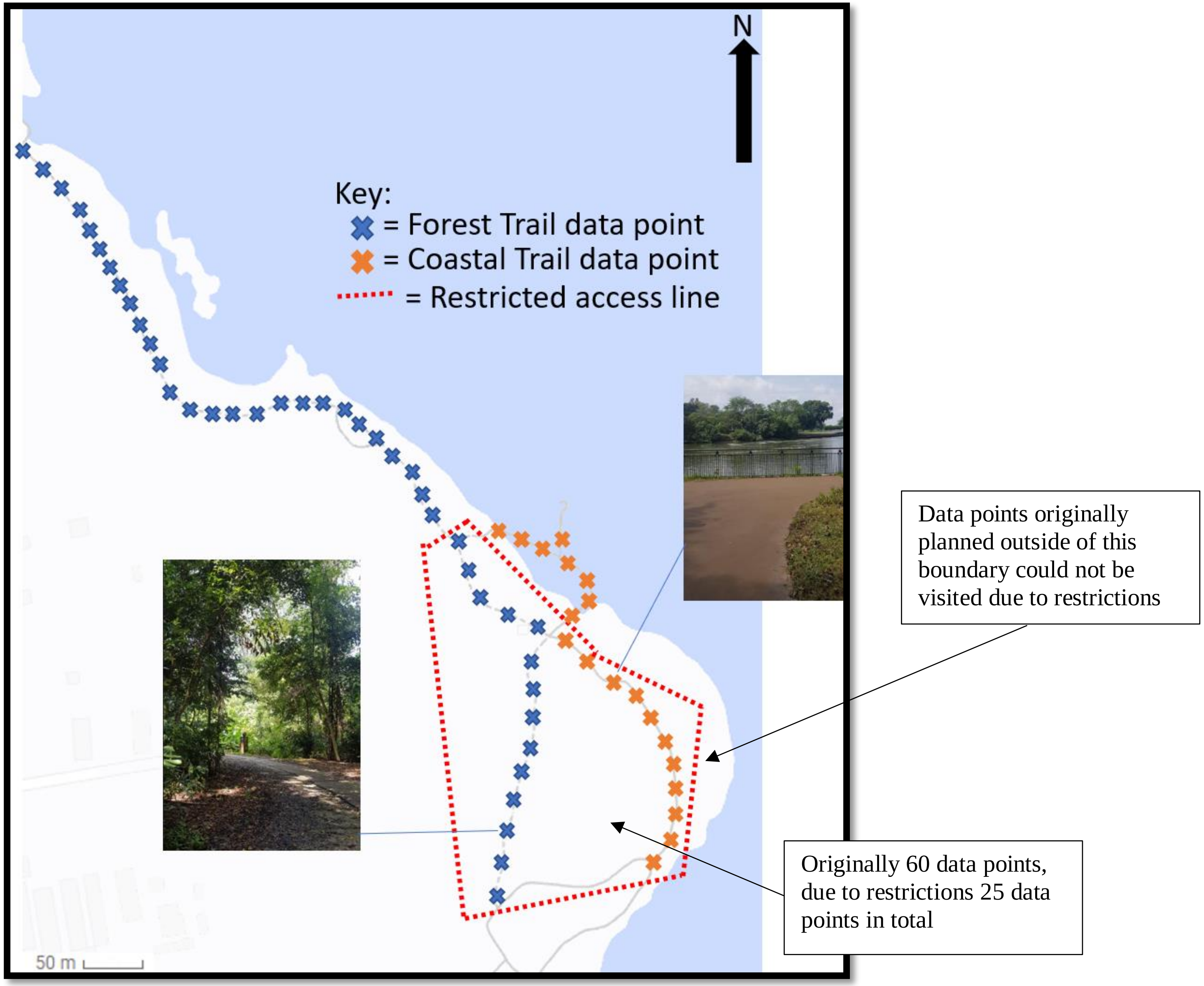

Figure 23 - Transect map of SBWR, adapted from GoogleMyMaps, pictures by candidate

6. Results and Analysis

Since data is univariate, conclusions drawn will originate from contrasting measures of central tendency and dispersion. Box and Whisker diagrams and histograms are used for quartile and distribution analysis. However, because intended data was not completely collected, proportions are investigated for fairness, represented through pie, line, and waffle charts. Statistical tests will be conducted in situations where significance of relationships present is seemingly doubtful, to see if numerical similarity of two data sets that could have arisen by chance. To avoid calculation errors, as data sets are large, all calculations will be done on Microsoft Excel.

6.1. Hypothesis 1: Temperature at DCSG is more numerically like JE than SBWR

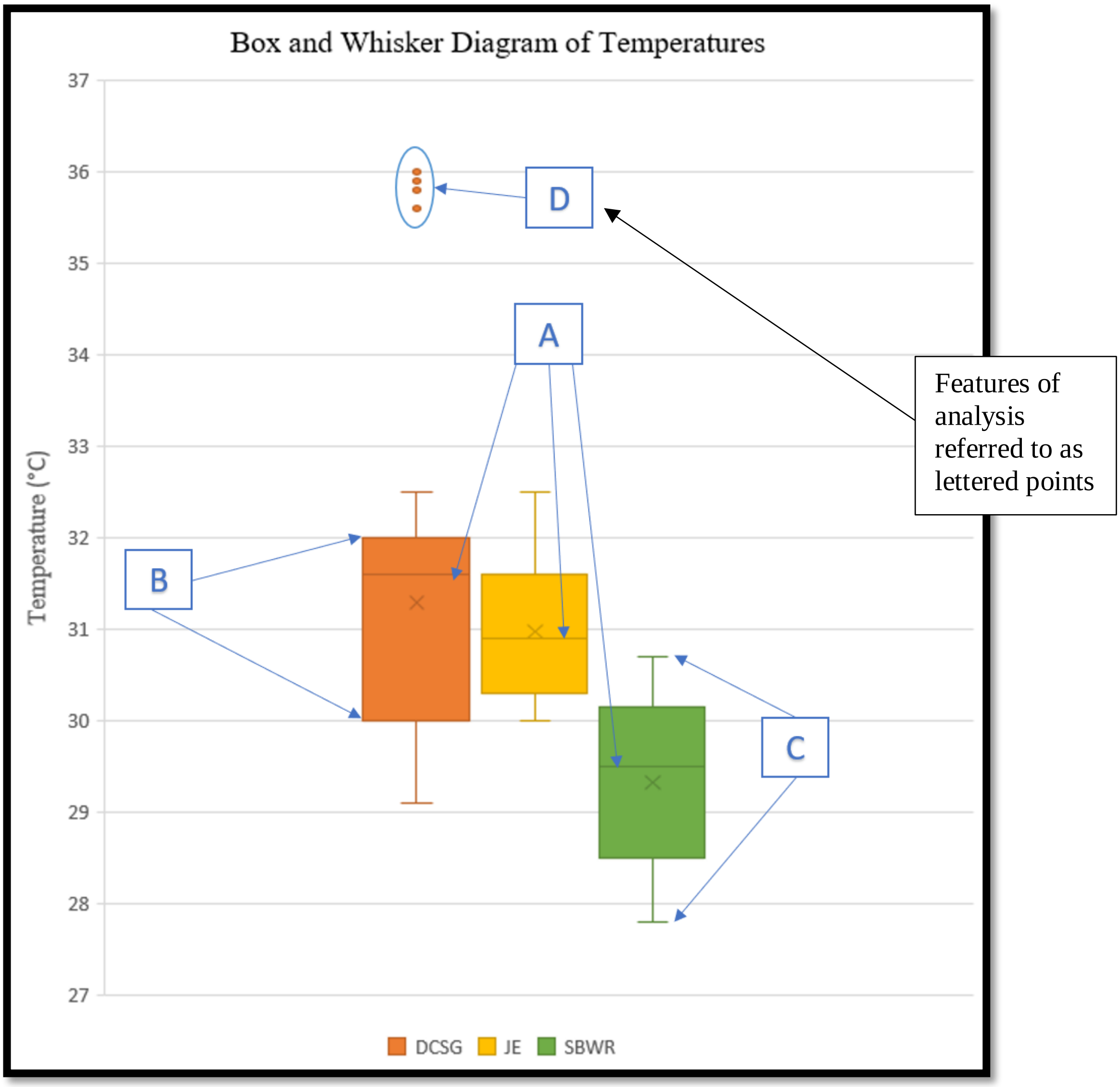

Figure 24 - Box and Whisker Diagram of Temperature at the 3 sites

‘A’ refers to median temperature values of DCSG (orange) and JE (yellow) being closer than DCSG and SBWR (green). Suggesting JE and DCSG share similar “middle" value. DCSG possesses a negative skew, as the median is closer to the upper quartile, caused by data points clustering there in the distribution. Median not heavily influenced by skewed data points like the mean in non-Gaussian distributions, hence better in this case.

‘B’ illustrates DCSG’s interquartile range almost entirely encapsulating JE’s range suggesting numerical similarities. Initially suggesting, even part of DCSG could have an urban microclimate. DCSG overlaps negligibly with SBWR suggesting numerical dissimilarity.

JE and DCSG may have land with low albedos; these surfaces absorb more heat radiation. Fig.10 suggests 0.05 albedo is observed on asphalt and 0.20 on brick. Asphalt roads are seen in JE (fig.26) and brick walls in DCSG (fig.25). Comparatively, a high albedo would be a white reflective surface, at 0.50-0.60, which mostly reflects solar radiation than absorb it as heat.

Figure 25 - Picture of the side of a building in DCSG by candidate

Figure 26 - Picture of road in JE by candidate

‘D’ shows outlying values, attributed to incorrect method. The thermometer may have been close to the ground, recording surface instead of air temperature, likely it is hypersensitive. Furthermore, these readings were taken on an elevated and open platform (tennis courts), the only of its kind at DCSG without vegetation.

‘C’ shows minimum and maximum values of the box plots. Seemingly large, suggesting data could be far from the mean; standard deviation provides a quantitative measure of spread (equation 1).

<u>Standard deviation formula:</u>

$$\sigma = \sqrt{\frac{\sum (\bar{x} + x)^2}{n}}$$

$\sum (\bar{x} + x)^2 = sum\ of\ squared\ differences\ between\ mean\ value\ and\ data\ set\ value$

$n = number\ of\ values\ in\ data\ set$

$\sigma = standard\ deviation$

units: arbitrary units

Equation 1 - Formula for Standard Deviation (RevisionMaths)

Standard deviation for DCSG is 1.78, 0.74 for JE and 1.38 for SBWR. DCSG is most spread out of all 3 data sets, a value of almost 2°C gives rise to believing multiple microclimates exist in DCSG's microclimate, like "fine-scale microclimatic variation" (Murdock) in literature, where microclimates exist in different areas of the microclimate on a temporal and spatial level, suggesting DCSG is not restricted to one classification.

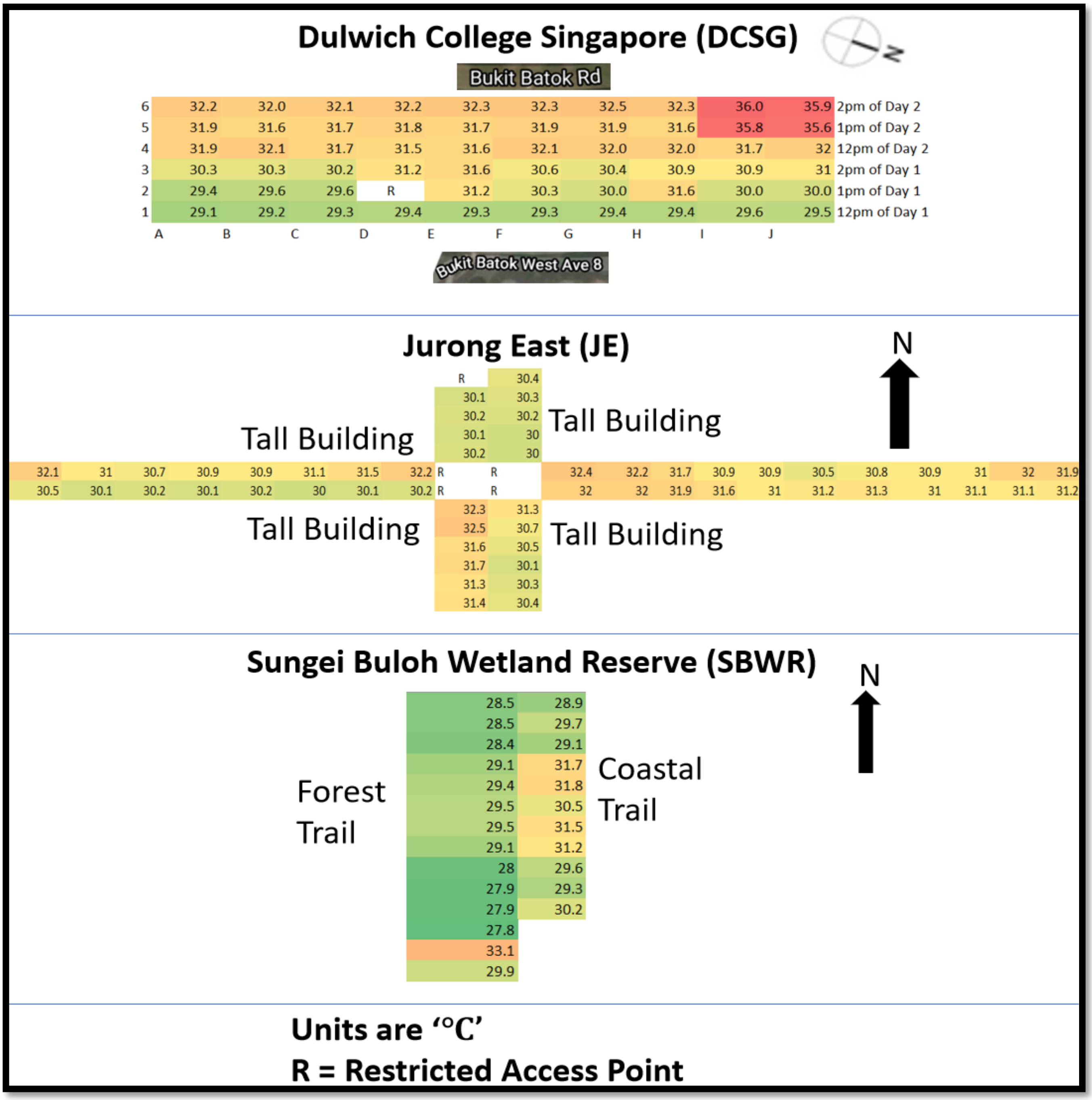

Figure 27 - Simplified choropleth map of temperatures in DCSG, JE and SBWR

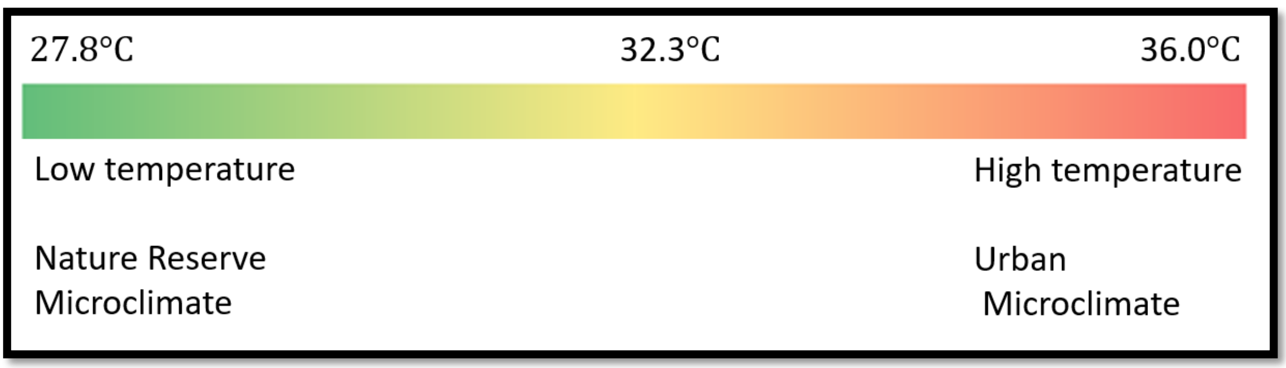

Figure 28 - Scale representative of the magnitude order of temperatures for fig. 27

Fig.27 for DCSG shows with increasing y-coordinate value, greater temperatures and urban microclimatic character are seen. Temporally speaking, data was collected on 2 consecutive days than 1, implying the second day was hotter. However, gradients of rows 1-3 illustrate increasing temperature with time, on roads either side of DCSG may have gotten busier, as parents drive to pick up children at 3.30pm, creating heat. JE benchmarks the urban microclimate, Wong et al.'s 24-hour temperature plot of JE (fig.15) dips, rather than increases, towards 3pm. This does not match the data collected for DCSG. Although literature placed an emphasis on temporal features, temperature patterns in DCSG may be more greatly attributed to spatial features.

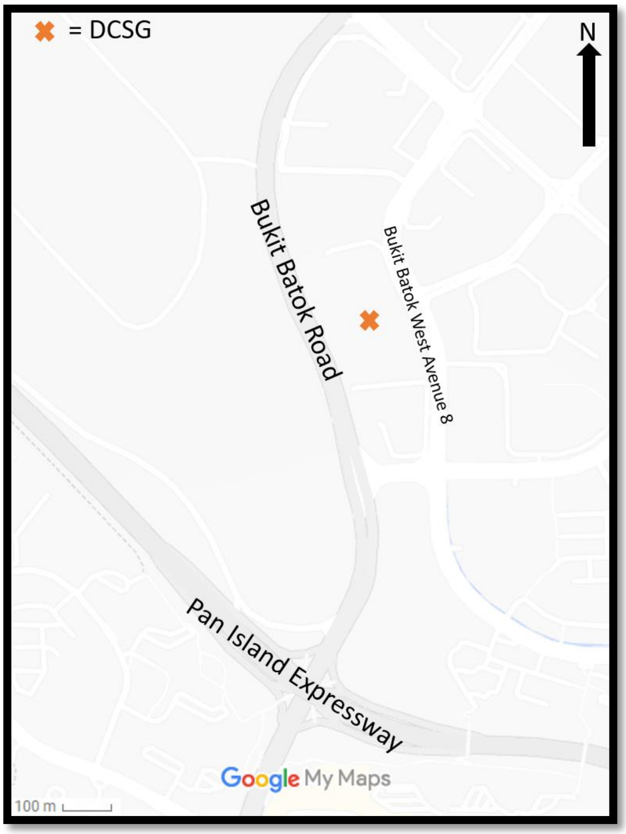

Figure 29 - Simple map showing roads near DCSG, adapted from (Google)

Fig.29 illustrates 3 roads in relation to DCSG, their differences are illustrated in figures 30 and 31. Pan Island Expressway is the only expressway to serve the length of the entire island, innumerable cars use it daily. These vehicles use the arteriole road (Bukit Batok Road) to reach DCSG and neighbouring land uses. Anthropogenic heat produced at Bukit Batok West Avenue 8 will be less as it is a slow (school) zone. Proportionally, ostensibly, there is greater usage of the other 2 roads. Therefore, the colour gradient of temperatures for DCSG on fig.27 could be attributed to greater anthropogenic heat on the expressway and arterial road.

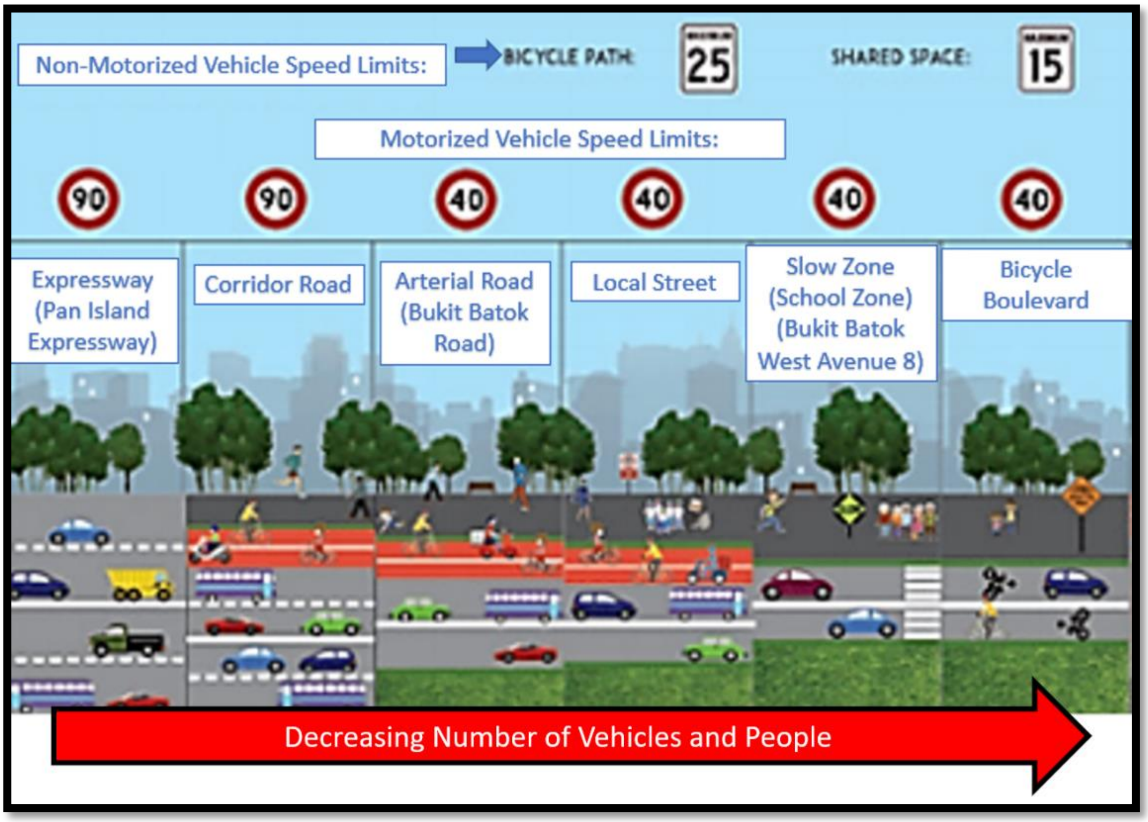

Figure 30 - Illustration representing road types in Singapore, adapted from Ho and Isaac

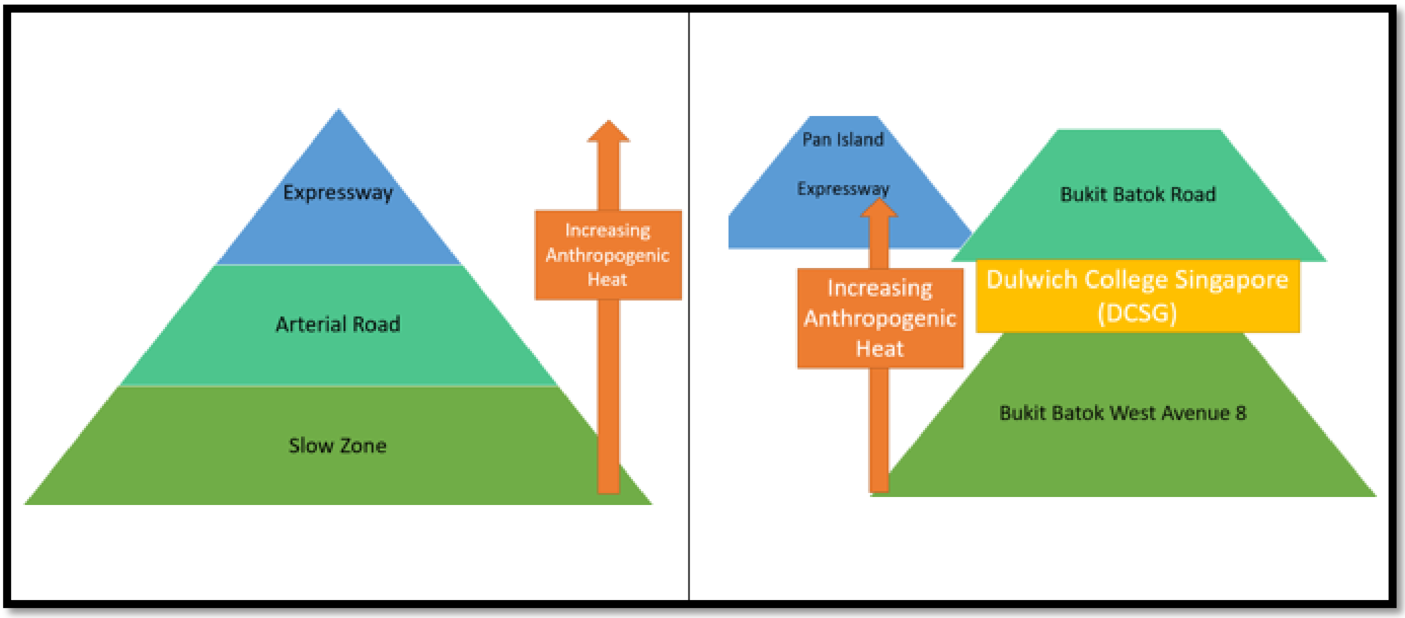

Figure 31 - Illustration of the hierarchy of roads (left) and hierarchy of roads in relation to DCSG (right)by candidate

Because greater urban microclimate character was seen in the temperature, this hypothesis is accepted.

6.2. Hypothesis 2: RH% at DCSG is more numerically like JE than SBWR

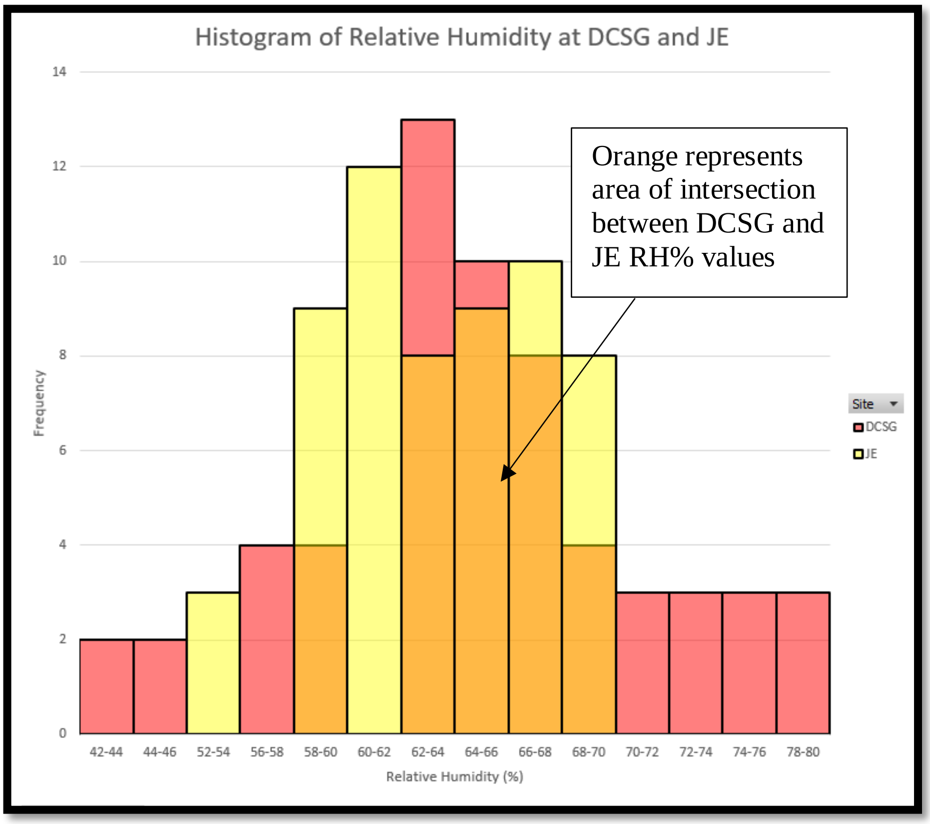

Figure 32 - Histogram of RH% at DCSG and JE

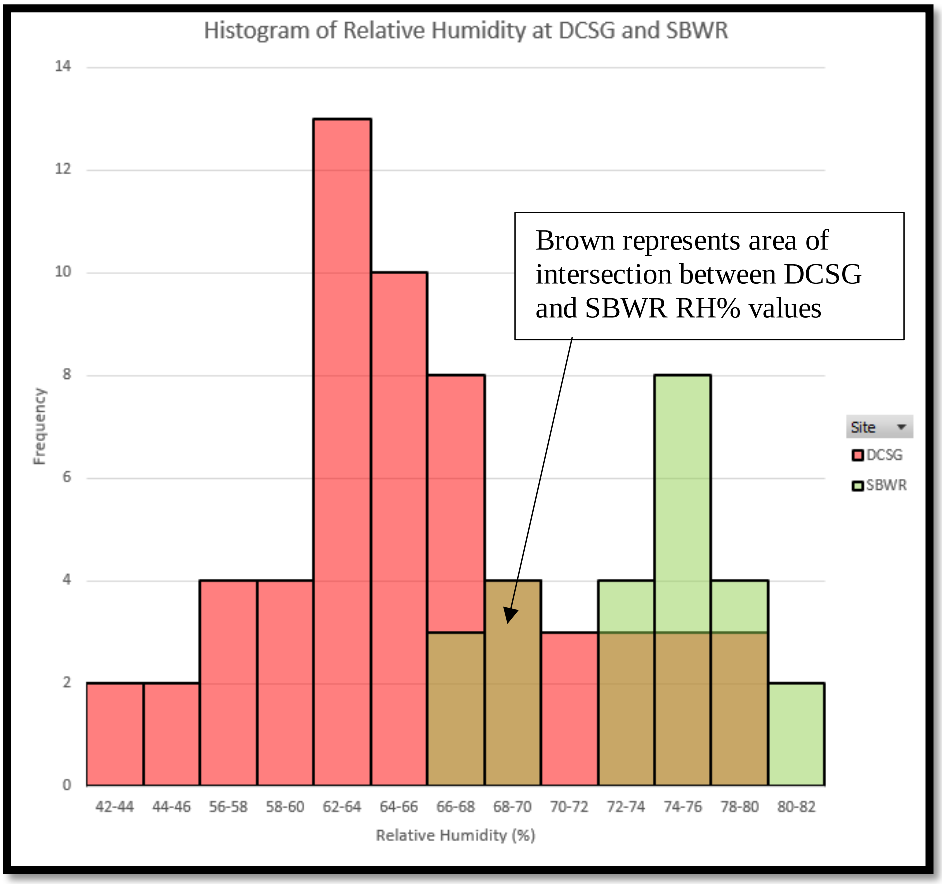

Figure 33 - Histogram of RH% at DCSG and SBWR

Overlap between DCSG and JE is greater than DCSG and SBWR, suggesting greater numerical similarity. However, because SBWR has less data points, the conclusion cannot stand unless proportions are compared.

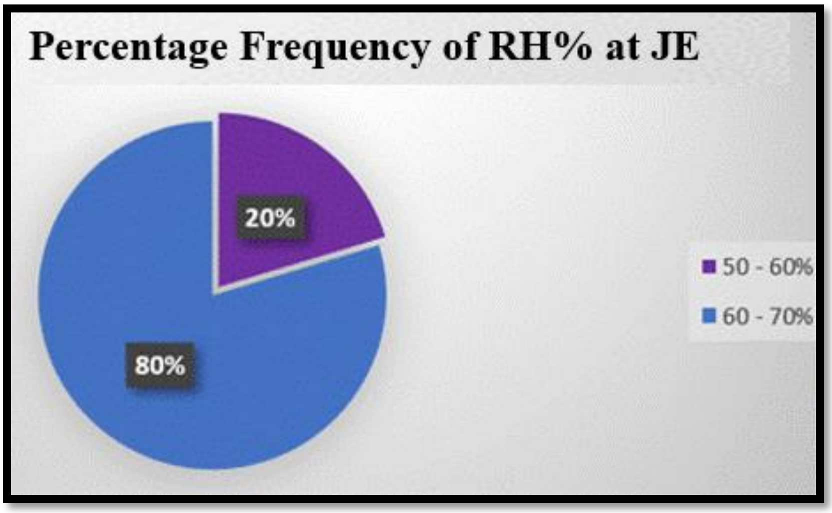

Figure 34 - Pie chart of RH% at JE

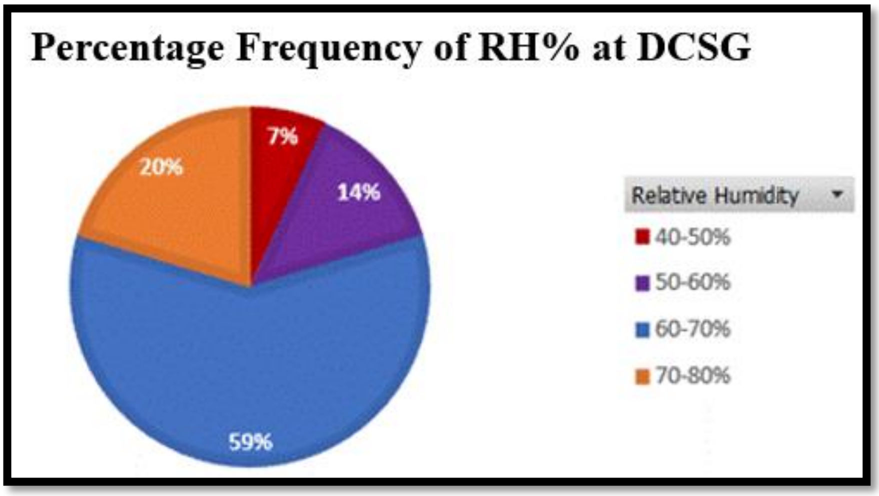

Figure 35 - Pie chart of RH% at DCSG

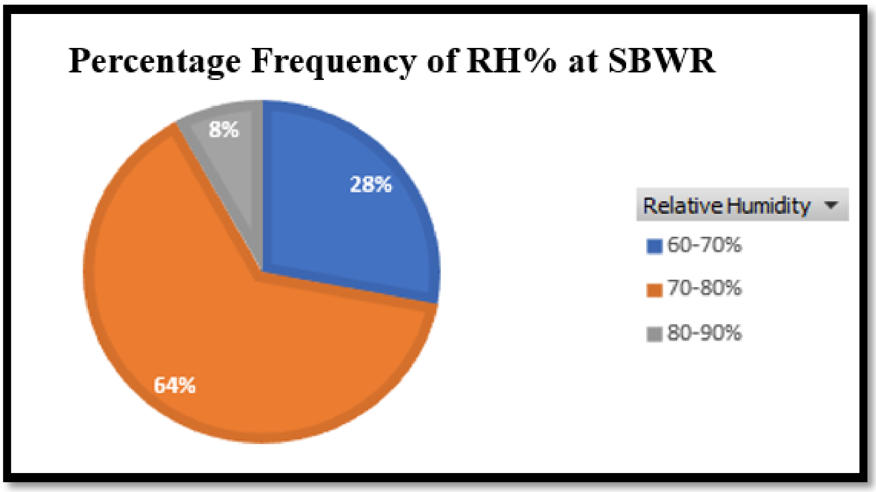

Figure 36 - Pie chart of RH% at SBWR

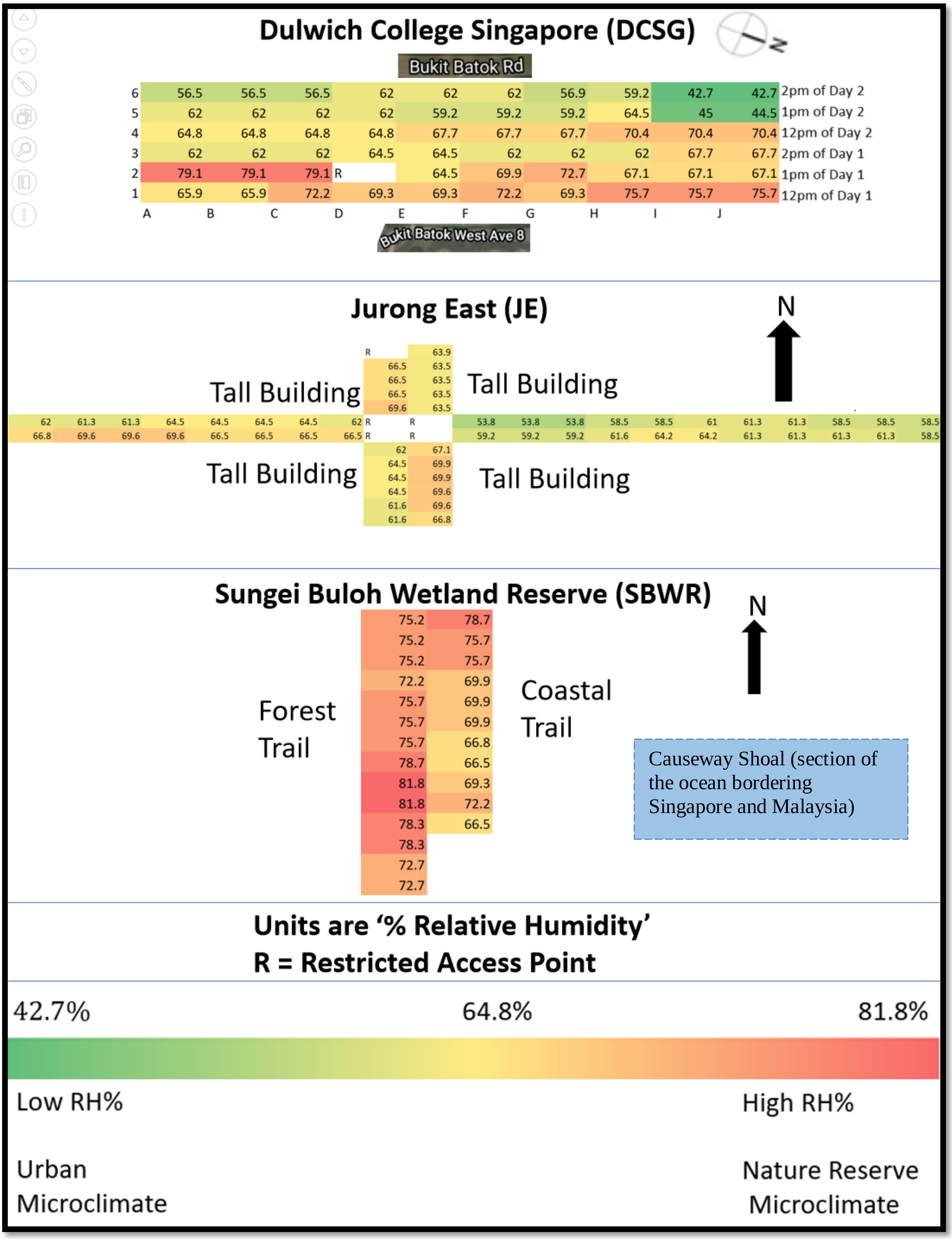

Figure 37 - Simplified choropleth map of RH% in DCSG, JE and SBWR

Figs.34-36 show DCSG shares the greatest proportions of RH% with JE than SBWR. JE is within DCSG's RH% range. JE and DCSG share more than half of their values in the 60–70 RH% band. 64% of SBWR's values are in the 70-80 RH% band, but DCSG only has 20% of its values there. in 50-60 RH%, where DCSG has 14% and JE has 20% of their values respectively, SBWR does not have any values in this band.

Since Nature Reserves' vegetation structure are based off existing rainforests, cumulative evapotranspiration cycles for vegetation caused high humidity to exist at SBWR. Considering spatial context of the coastal trail (fig.37), the site's contiguousness with the Causeway Shoal (section of the ocean) may have caused high RH% due to concurrent winds evaporating water and transporting water vapour to land.

Aspects of both microclimate types are seen in DCSG in fig.37. The lurched nature of data at all 3 sites is due to the lack of variation in readings on the wet-dry bulb. Minute discrepancies cannot be identified, hence less of a gradient is observed than fig.27, owing to dearth in precision. The fall in temperature causes a rise in RH% if water vapour content and pressure is static, hence an inverse gradient of DCSG in fig.27 was produced.

There is a seemingly even divide between urban and nature reserve microclimatic character because some values in JE and SBWR overlap, making differentiation difficult, rows 1-2 are like SBWR, whilst 3-6 are like JE. However, it should be considered that fig.37 perhaps purports the numerical significance of the sites through similarities in data point colour.

Conclusively, the presented quantitative evidence suggests RH% of DCSG is more numerically like JE than SBWR, H_2 is accepted. Accepting this does not disregard the similarity between DCSG and SBWR, it is simply less than JE and DCSG's similarity.

6.3. Hypothesis 3: Light intensity at DCSG is more numerically like JE than SBWR

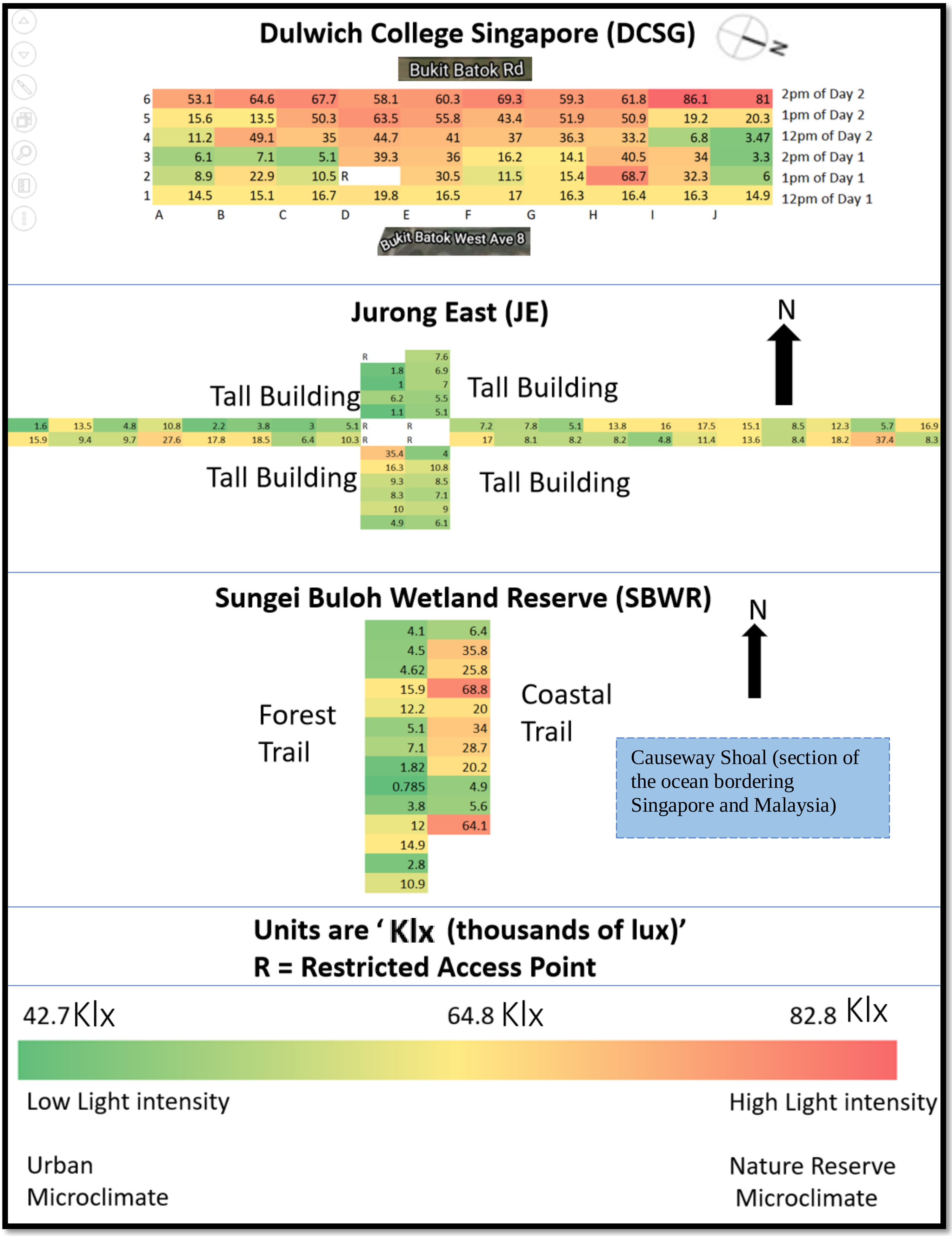

Figure 38 - Simplified choropleth map of Light intensity in DCSG, JE and SBWR

Fig.38 illustrates spatial distribution of light intensity. Rows 4-6 are largely open space, including the rugby field, tennis courts and aquatic centre, the lack of cover causes elevated light intensity. Besides that, similarity in shading makes distinguishing JE and SBWR difficult, rising questionability on their significant difference. However, proportions may differentiate them.

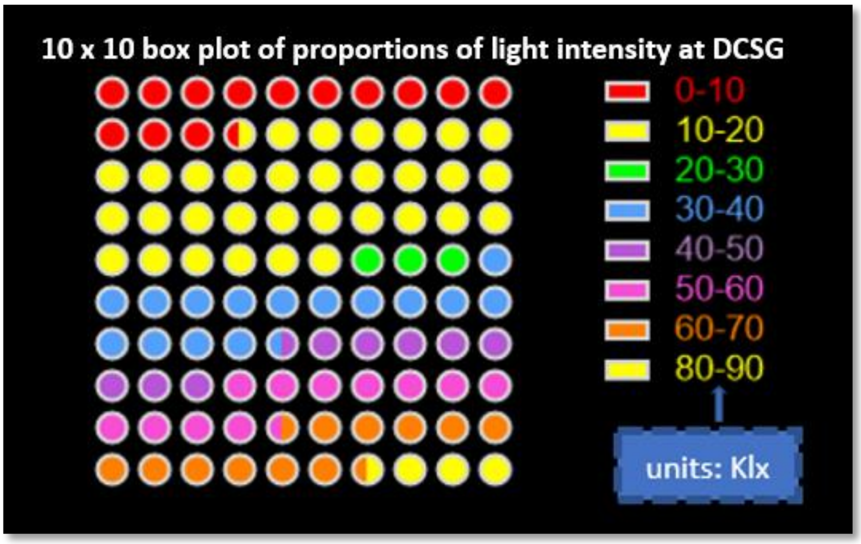

Figure 40 - 10 x 10 box plot of proportions of light intensity at DCSG (units: Klx)

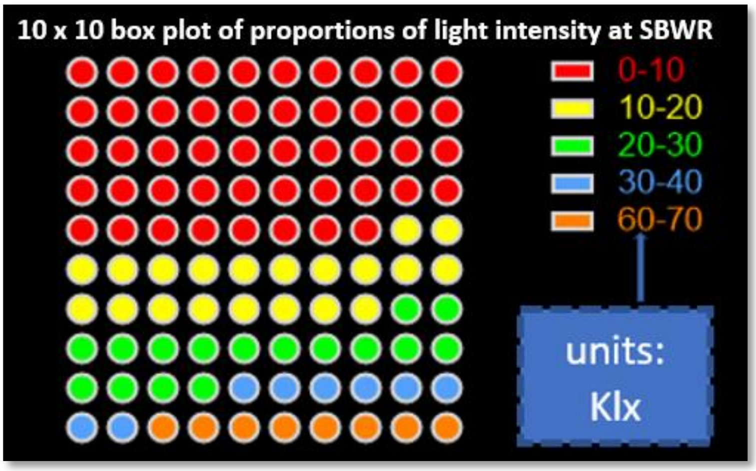

Figure 39 - 10 x 10 box plot of proportions of light intensity at SBWR (units: Klx)

Figure 41 - 10 x 10 box plot of proportions of light intensity at JE (units: Klx)

0-10Klx and 10-20Klx bands are similar for SBWR and JE are similar shown by the red and yellow dots, numerically similarity is hard to distinguish and superficially implies no significant difference between JE and SBWR. Parametric tests can be used to see for significant difference. The tests assume distribution as normal, not skewed. 'Central limit theorem', which suggests a normal distribution will exist if there are more than 30 data points (Ganti) in a data set, cannot be assumed as SBWR has 25 points. Below, a logarithmic transformation of every data point aims to create Gaussian distribution (shifting skewness to 0).

Skewness:

$$\text{Skewness} = \frac{\sum_i^N (X_i - \bar{X})^3}{(N-1) * \sigma^3}$$

$$X_i = Random\ Data\ Point$$

$$\bar{X} = Mean\ of\ Data\ Points$$

$$N = Number\ of\ Data\ Points$$

$$\sigma = Standard\ Deviation$$

Equation 2 - Skewness

Logarithmic Transformation:

$$Log_{10}(X_i) = Logarithm\ to\ Base\ 10$$

Equation 3 - Logarithmic transformation

		Skewness of Data at Sites		
		DCSG	JE	SBWR
Data under A/B conditions	A = Natural Distribution	0.569	1.854	1.845
	B = Logarithmic Transformation	-0.514	-0.686	-0.143

Table 4 - Results table for skewness

Though the skewness became negative, the modulus values became closer to zero making the data sets more "Gaussian". Comparing means of independent samples requires the 't-test'. An equal or unequal variance between data sets is determined to find the correct t-test. Table 5 (full calculation in appendix B) below shows an unequal variance between JE and SBWR.

	JURONG EAST (JE)	SUNGEI BULOH WETLAND RESERVE (SBWR)
Number of data points	n 59	25
Mean values	$\bar{x}$ = 0.90563	$\bar{y}$ = 0.98797
Sum of squared differences		
	$\sum$ = 6.02324	$\sum$ = 5.52512
Degrees of Freedom		
	n - 1 = 58	n - 1 = 24
Variance		
	$s_x^2 = \frac{\sum(x-\bar{x})^2}{n-1}$ = 0.103849004	$s_y^2 = \frac{\sum(y-\bar{y})^2}{n-1}$ = 0.230213238
F value (larger variance divided by smaller variance)	F = s_y^2/s_x^2 = 2.216807369	
Degrees of freedom 1:	24	
Degrees of freedom 2:	58	
Probability level:	0.05	
Calculate!		
Critical F-value:	1.70647557	
F(stat) =	2.21681	
F(crit.)=	1.70648	
F(crit.) < F(stat.)		
Unequal variance between groups		

Table 5 - Table of results for calculating variance type through F-value calculation for JE and SBWR's light intensity, critical F-value from Soper, formulae from O'Loughlin

The respective null and alternate hypotheses for the unequal variance t-test at Alpha value 0.05 and two tailed:

H_0: Mean of JE = Mean of SBWR

H_A: Mean of JE ≠ Mean of SBWR

Table 6 shows the null hypothesis (**H_0**) is not rejected as the T(stat) does not fall into the reject region, therefore there is no significant difference between the means of JE and SBWR. The t-test shows there is no statistical significance between JE and SBWR. This means the overall hypotheses (H_3) is rejected, as differences in means could have arisen by chance. This outcome may have been reached because the data was still skewed after log transformation.

T-statistic		
$t = \frac{(\bar{x}-\bar{y})}{\sqrt{\left(\frac{S_x^2}{n_x}+\frac{S_y^2}{n_y}\right)}} =$	$t = \frac{(0.905625541 - 0.987966239)}{\sqrt{\left(\frac{0.103849004}{59}+\frac{0.230213238}{25}\right)}} =$	**-0.78621**
Degrees of Freedom		
$df = \frac{\left(\frac{s_x^2}{n_x}+\frac{s_y^2}{n_y}\right)^2}{\frac{(s_x^2/n_x)^2}{n_x-1}+\frac{(s_y^2/n_y)^2}{n_y-1}} =$	$\frac{\left(\frac{0.103849004171196}{59}+\frac{0.230213237701711}{25}\right)^2}{\frac{(0.001760153)^2}{59-1}+\frac{(0.00920853)^2}{25-1}} =$	**33.54**
Critical value at alpha level 0.05 =	T(crit) = 2.042 T(stat) = -0.78	
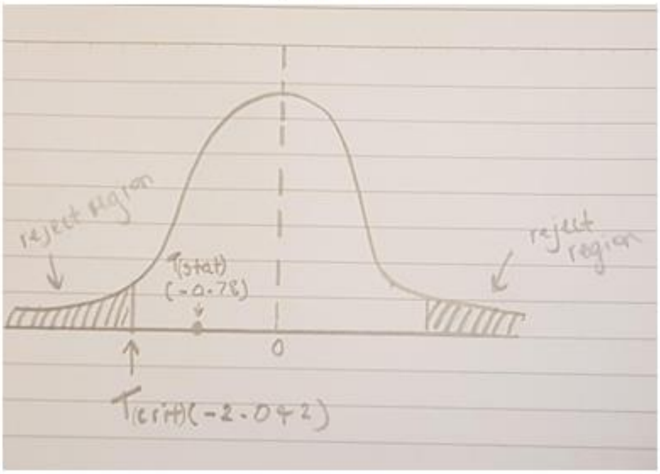		
T(stat) does not fall into the reject region ∴ H0 is not rejected		

Found through table in appendix C

Table 6 - t-test for JE and SBWR for light intensity data, formulae from O'Loughlin

Fig.38's spatial distribution corroborates this by showing light intensity increases with time and distance towards the main road, whilst JE nor SBWR present results indicating a shared microclimate. Light intensity intends to communicate the levels of pollution from combustive processes, as microscopic particles block sunlight from hitting the floor, attributed to an urban microclimate. However, fig.42 models light intensity of DCSG on the days of data collection, suggesting time plays a role. From 12pm to 2pm, the shadow casted on DCSG weakens suggesting the diurnal earth rotation causes the origin of sunlight to shift from South to North, this may have been why light intensity increased from rows 1 to 6 on fig.38.

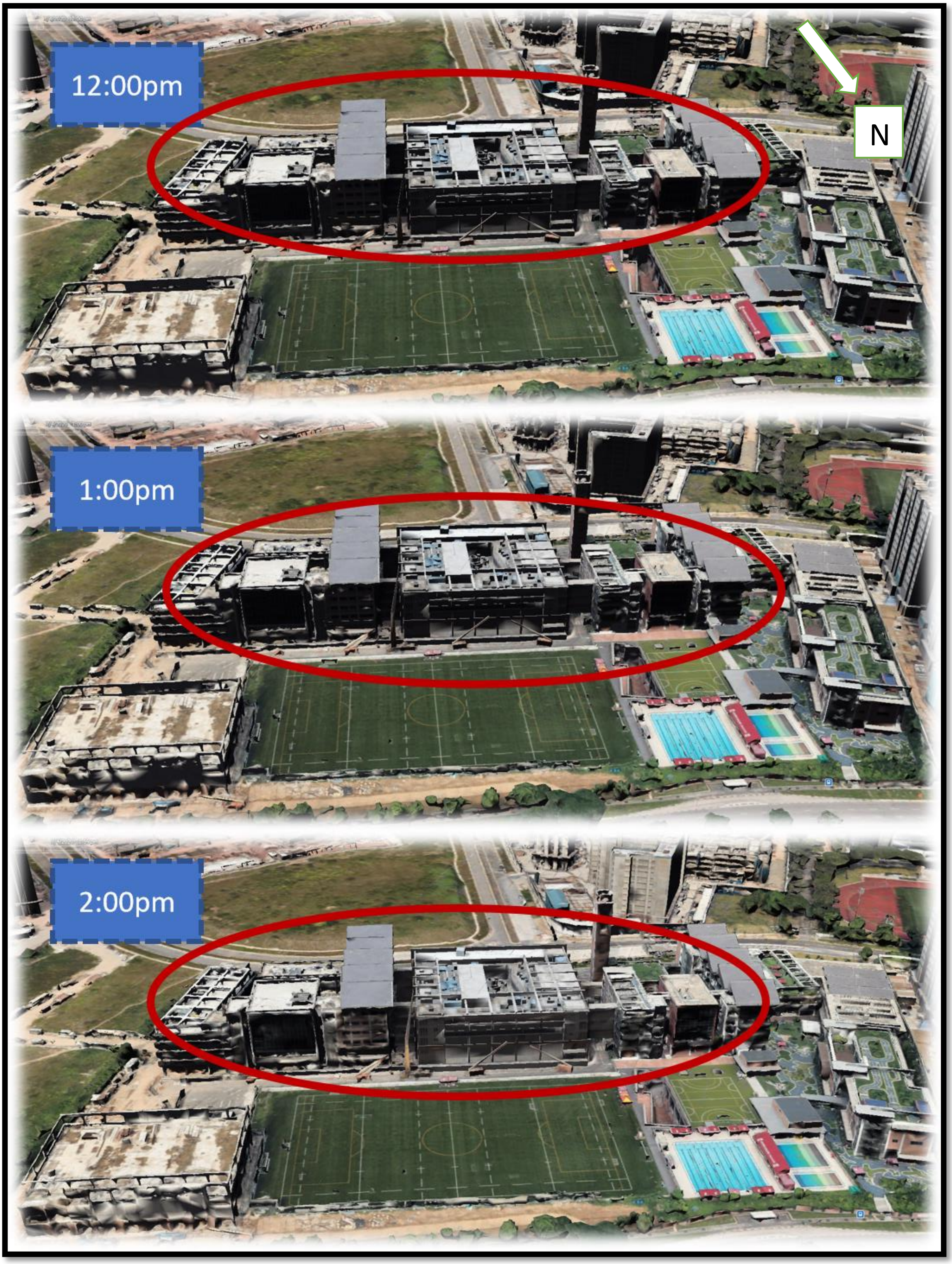

Figure 41 - Solar radiance over time at DCSG, adapted from screenshots of simulations in Google Earth

6.4. Hypothesis 4: Wind speed at DCSG is more numerically like JE than SBWR

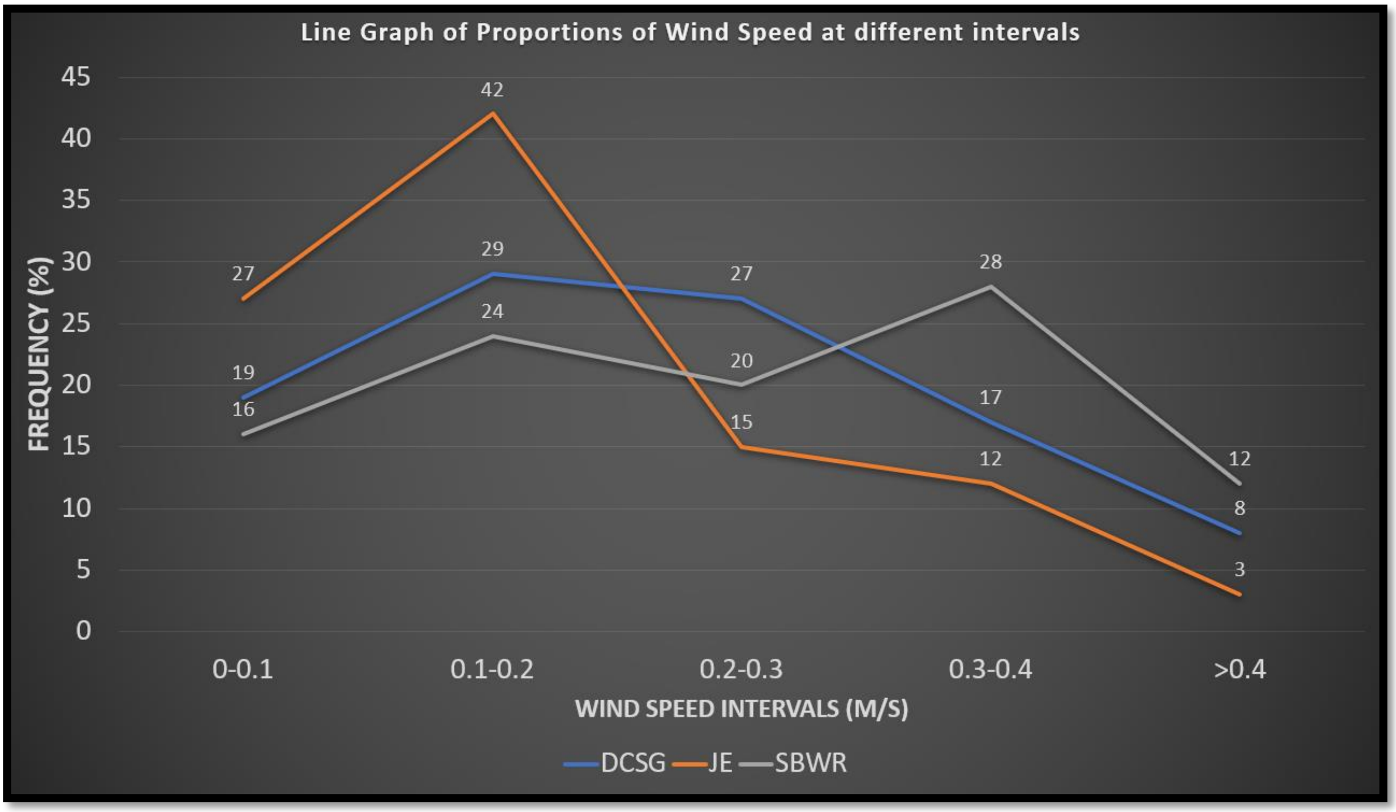

Figure 42 - Line graph of proportions of wind speed at different intervals

Points on the graph represent proportions at different wind speeds for each site. DCSG and SBWR's trendlines differ least in frequency percentage between them suggesting numerical similarity. JE's wind speeds are concentrated on 0-0.2m/s whilst both SBWR and DCSG both follow the same distribution apart from 0.3-0.4m/s. Rather than using covered walkways, DCSG uses vegetation, allowing wind to pass whilst keeping students out of the sunlight (fig.45). Fig.44 highlights D2/3 and F2/3 as potential outliers. These are higher than surrounding values, taking place between buildings. The higher wind speed may be due to the venturi effect - "When winds are funnelled through a relatively small opening" (Spirn). Buildings act as walls of a narrow containers (fig.46), over observed in urban areas due to tight partitions, thereby supporting urban microclimate existence to some extent. However, the flexible structure of vegetation in SBWR and DCSG provides evidence for existing greater numerical likeliness, hence the hypotheses is rejected.

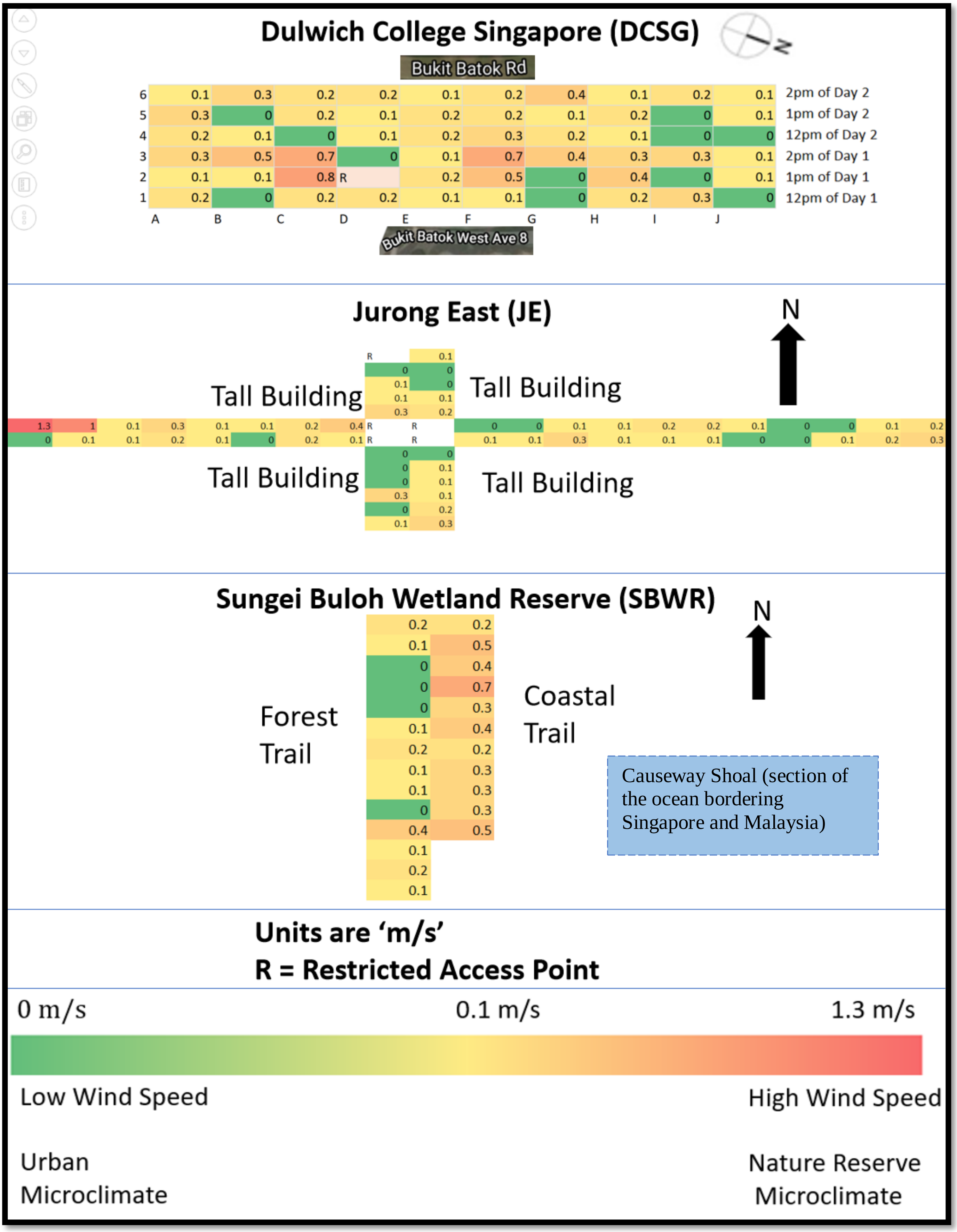

Figure 43 - Simplified choropleth map of Wind Speed in DCSG, JE and SBWR

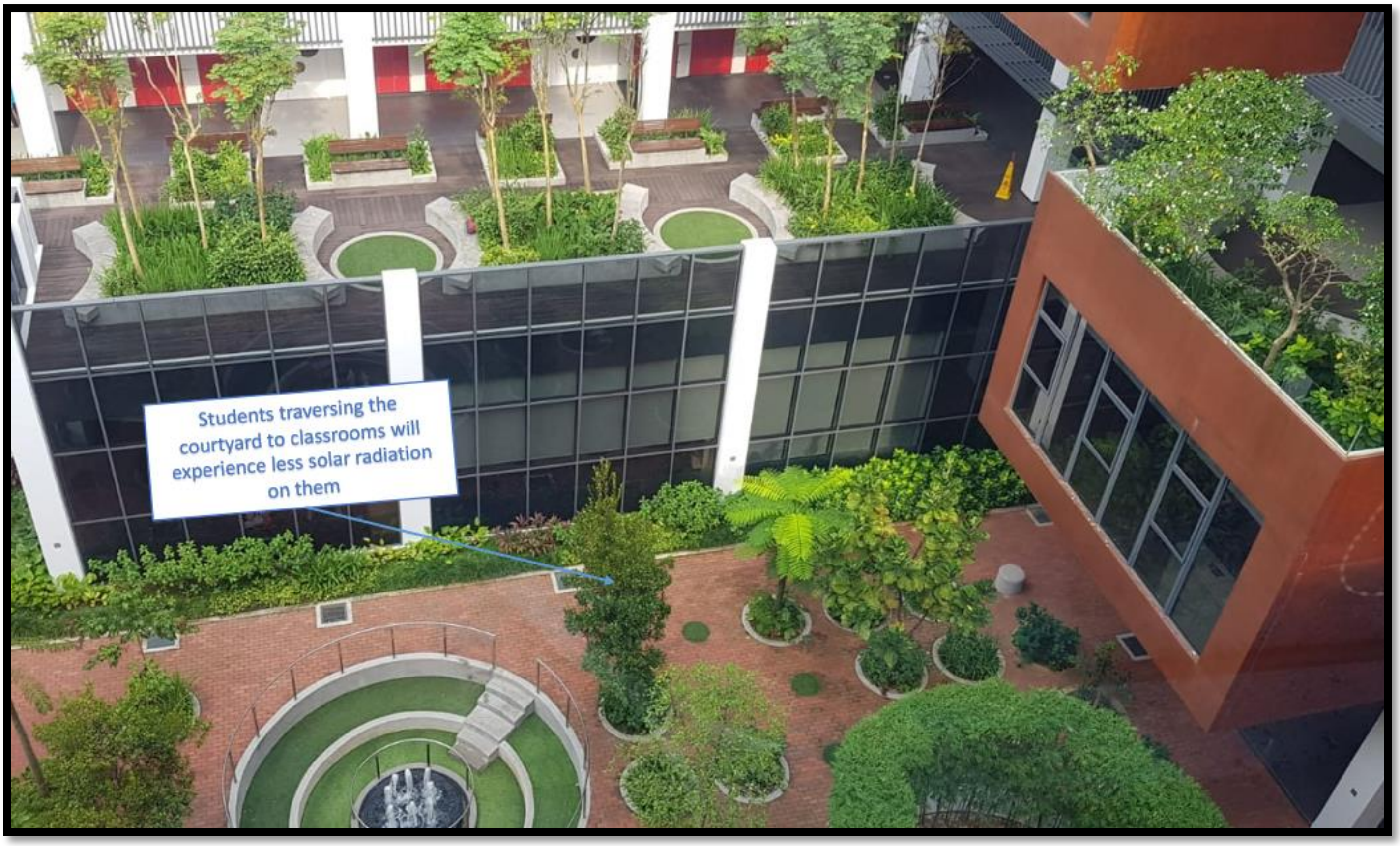

Figure 44 - Photograph of the Courtyard by candidate

Figure 45 – Photograph of Point D2 on fig.44 by candidate

7. Evaluation

Strength	Reasoning
Sampling	Systematic sampling covering all DCSG allowed aggregate patterns of data to be observed.
Spatial consideration	Precise, allowing for observations of smaller variation.
Using local papers	Methodology was informed of Singaporean caveats and avoided limiting approaches.

Table 7 - Strengths

Weakness	Improvement
Wind speed - detecting small changes were difficult, the margin of error likely high	Causes of microclimates, like albedo, can be measured to find relationships between causes and meteorological effects.
Not enough data – SBWR only had 25 data points	Using an alternative nature reserve with less restricted areas
Urban microclimate site - Often DCSG showed more urban microclimate character than JE	Orchard Road primary CBD could be compared, may show a better urban microclimate
Temporal data – times were only recorded for the transects of data as a whole	Record the time for every data point, temporal changes in microclimate can be observed

Table 8 – Weaknesses and respective improvements

8. Conclusion

2 of 4 hypotheses in support of DCSG's urban microclimate were accepted, from numerical similarity between sites alone the extent at which DCSG possesses an urban microclimate is equal to a nature reserve microclimate. Upon further inspection, one was rejected in support of the nature reserve microclimate, another due to statistical insignificance. Considering that a hypothesis rejection based on statistical insignificance is not enough to rule out the possibility of either microclimate, omitting this factor, the conclusion favours the urban microclimate. Therefore, the extent at which DCSG possesses an urban microclimate is **slightly** greater than a nature reserve microclimate, suggesting DCSG's population is at moderate risk from heatwaves. Spatial distributions for DCSG persistently displayed a steep gradient of values from the West to East (fig.21) or top to bottom, showing the shift from urban to nature reserve microclimate, hence efforts to combat the urban microclimate can be focused on certain areas. Considering the implications of this conclusion in a wider context and Murdoch's "fine-scale microclimatic variation", categorically stating DCSG possesses one microclimate over the other does not pay homage to data (of a less degree) stating otherwise. The alternative argument could be made that comparing thermal comfort or data gauging the local population's opinions is the only way to find out if microclimates are similar in effect, however level of bias associated with this high, potentially misrepresenting the true conclusion. Quantitative meteorological data (apart from numerically transformed qualitative data) contains little degree of bias, making this conclusion viable. Though not in the hypotheses, analyzing photographs and spatial and temporal dynamics, contributed to a holistic approach in answering this research question as they are key contextual markers in geography; they invigorated paradigm shifts in this paper, making them an important addition to hypothesis acceptance/rejection and therefore the overall conclusion. The methodology was suitable for managing the scale and volume of data collection.

This investigation brought about the deeper understanding that microclimates are not static, and will alter with time, space, and human interactions with the environment. From a researcher's perspective, seeing that the initial hypotheses that were in full support of an urban microclimate were disproved, provided a glimpse into the impact of incorporating greenery and a biophilic design on microclimates in the larger urban environment of Singapore. This leads to a potential adaptation to the inquiry, investigating causes instead of meteorological consequences of microclimates.

9. **<u>Bibliography</u>**

Albahae, Ms. *Land Use Models*. 2018. LEWIS HISTORICAL SOCIETY AP HUMAN GEOGRAPHY. PDF document. Accessed 8 September 2020. <https://albahaeaphg.files.wordpress.com/2018/04/the-urban-city-models-and-more-handout.pdf>.

Balázs, Bernadett, et al. *Micro-climate in a High-Rise Residential Development in Singapore*. 26 April 2016. Website. Accessed 21 June 2020. <https://www.fas.nus.edu.sg/srn/archives/52257>.

Burdett, Matthew. *Urban microclimates: causes*. 4 November 2019. Website. Accessed 5 June 2020. <https://geographycasestudy.com/urban-microclimates-causes/>.

Candidate. *Data Collection Photographs*. Dulwich College Singapore, Singapore. Accessed July 2020.

Dulwich College Singapore. *Private Tour Graphics* . Singapore, 2020. Website. Accessed 16 June 2020. <https://singapore.dulwich.org/private-tour>.

Ganti, Akhilesh. *Central Limit Theorem (CLT)*. 13 September 2019. Dotdash . Website . Accessed 13 October 2020. <https://www.investopedia.com/terms/c/central_limit_theorem.asp>.

Gerstman, B. Burt. "t Table." 14 July 2007. *StatPrimer* . PDF. Accessed 13 October 2020. <https://www.sjsu.edu/faculty/gerstman/StatPrimer/t-table.pdf>.

Godfrey, Brian J. "The Geography of James E. Vance Jr. (1925-1999)." *Geographical Review* 89.4 (1999): 580-589. PDF. Accessed 10 July 2020. <www.jstor.org/stable/216103>.

Google Earth. *Google Earth*. Google . 2020. Website . Accessed January - October 2020.

Google. "GoogleMyMaps." n.d. Website. <https://www.google.com.sg/maps/d/u/0/>. Accessed January - October 2020

Hall, Sharon J., Jenni Learned and Benjamin Lyle Ruddell. *Convergence of microclimate in residential landscapes across diverse cities in the United States*. October 2015. PDF. Accessed 19 September 2020. <https://www.researchgate.net/publication/283081807_Convergence_of_microclimate_in_residential_landscapes_across_diverse_cities_in_the_United_States>.

Ho, Cherub and Martha Isaacs. *Figure 18: Singapore's new street design guidelines . Centre for LiveableCities Singapore* . Singapore , n.d. Illustration . Accessed 17 October 2020. <https://www.clc.gov.sg/docs/default-source/commentaries/bc-2018-05-multimodal-streets-for-all.pdf>.

International Schools Database. *Dulwich College (Singapore)*. 2020. International Schools Database. Website. Accessed 8 October 2020. <https://www.international-schools-database.com/in/singapore/dulwich-college-singapore>.

Jacobs, Brent Charles and Candice Delaney. *Adapting to urban heat in Penrith*. Technical Report. University of Technology Sydney. Sydney, 2015. PDF. Accessed 18 June 2020. <https://www.researchgate.net/publication/334067981_Adapting_to_urban_heat_in_Penrith>.

Jin, Hong, et al. "Assessing the Effects of Urban Morphology Parameters on Microclimate in Singapore to Control the Urban Heat Island Effect." *Sustainability* (2018): 1-16. PDF. Accessed 20 June 2020. <https://www.researchgate.net/publication/322519469_Assessing_the_Effects_of_Urban_Morphology_Parameters_on_Microclimate_in_Singapore_to_Control_the_Urban_Heat_Island_Effect>.

Kennard, Annajane. *Singapore*. 26 July 1999. Website . Accessed 1 July 2020. <https://www.britannica.com/place/Singapore>.

Koninck, Rodolphe De. "Singapore: A Global Strategic Location ." Koninck, Rodolphe De. *Singapore's Permanent Territorial Revolution: Fifty Years in Fifty Maps*. Singapore: NUS Press, 2017. 6-7. Ebook . Accessed 14 August 2020. <https://books.google.com.sg/books?id=T6zWDgAAQBAJ&printsec=frontcover&dq=singapore+map&hl=en&sa=X&ved=2ahUKEwi3oc_GoM_sAhWTj-YKHS4nBJEQ6AEwAnoECAQQAg#v=onepage&q&f=false>.

Landezine. *Dulwich College Singapore*. 2016. Website. Accessed 1 June 2020. <https://landezine-award.com/dulwich-college-singapore/>.

Li, Reuben, Dewen Chen and Guo Ann. *Mapping Potential Sea Level Rise in Singapore*. n.d. Website. Accessed 13 October 2020. <https://courses.nus.edu.sg/course/geowyc/course/GE3216/students/sea_level_rise/intro.htm>.

M.L. Parry, O.F. Canziani, J.P. Palutikof, P.J. van der Linden, C.E. Hanson, Eds. *Assessment of adaptation practices, options, constraints and capacity. In: Climate Change 2007: Impacts, Adaptation and Vulnerability. Contribution of Working Group II to the Fourth Assessment Report of the Intergovernmental Panel on Climate Change [M.L. Parry "et al.". Eds.]*. Ed. M. L. Parry, et al. Cambridge University Press, Cambridge, UK, and New York, N.Y., U.S.A., 2007. Accessed 16 October 2020. <http://www.ipcc.ch/publications_and_data/publications_ipcc_fourth_assessment_report_wg2_report_impacts_adaptation_and_vulnerability.htm>.

Met Office. "Microclimates." 2019. *metoffice.gov.uk*. Met Office . PDF. Accessed 27 June 2020. <https://www.metoffice.gov.uk/binaries/content/assets/metofficegovuk/pdf/research/library-and-archive/library/publications/factsheets/factsheet_14-microclimates.pdf>.

—. *Microclimates*. Fact Sheet . London, n.d. PDF. Accessed 9 October 2020. <https://www.metoffice.gov.uk/binaries/content/assets/metofficegovuk/pdf/research/library-and-archive/library/publications/factsheets/factsheet_14-microclimates.pdf>.

Meteorological Service Singapore. *Climate of Singapore*. 2010. Website. Accessed 13 June 2020. <http://www.weather.gov.sg/climate-climate-of-singapore/>.

Metlink. *URBAN HEAT ISLAND INTRODUCTION*. 2017. Website. Accessed 12 June 2020. <https://www.metlink.org/other-weather/urban-heat-islands/urban-heat-island-background/#:~:text=An%20urban%20heat%20island%20is,obvious%20when%20winds%20are%20weak.&text=The%20urban%20heat%20island%20effect%20is%20greatest%20in%20the%20Central%20Business%2>.

Morgan, Gary R. and Derek J. Staples. *The history of industrial marine fisheries in Southeast Asia*. BANGKOK: FOOD AND AGRICULTURE ORGANIZATION OF THE UNITED NATIONS, 2006. Accessed 1 October 2020. <http://www.fao.org/3/AG122E00.htm#Contents>.

Murdock, Courtney C. "Fine-scale variation in microclimate across an urban landscape shapes variation in mosquito population dynamics and the potential of Aedes albopictus to transmit arboviral disease." 2017. Website. 29 July 2020. <https://journals.plos.org/plosntds/article?id=10.1371/journal.pntd.0005640>.

Nagle, Garret and Briony Cooke. "OPTION G URBAN ENVIRONMENTS." Nagle, Garret and Briony Cooke. *Geogragphy - Course Companion*. 2nd. Oxford University Press, 2017. 330-386. Textbook. Accessed 1 June 2020.

Naim, Wan MOHD, Latif Abd Zulkiflee and Nasir Adawiyah Rabiatul. *Diurnal microclimate variations in tropical rainforest: Case study of Kuala Tahan, Pahang*. December 2012. Website. Accessed 14 June 2020. <researchgate.net/publication/261054625_Diurnal_microclimate_variations_in_tropical_rainforest_Case_study_of_Kuala_Tahan_Pahang>.

National Environment Agency. *WEATHERWISE SINGAPORE*. Meteorological Report. Singapore: NATIONAL ENVIRONMENTAL AGENCY, 2009. PDF. Accessed 10 June 2020. <https://www.nea.gov.sg/docs/default-source/resource/guidebook-on-climate-of-singapore.pdf>.

National Parks. *Flora and Fauna Web*. Prod. National Parks. Singapore, 2020. Website Database. Accessed 1 October 2020. <https://www.nparks.gov.sg/florafaunaweb>.

—. "MEDIA FACTSHEET D, Nature Parks as Buffer Parks." 2017. *National Parks* . PDF . Accessed 20 July 2020. <https://www.nparks.gov.sg/-/media/nparks-real-content/news/2017/windsor-nature-park/buffer-parks.pdf>.

—. *Parks & Nature Reserves*. 2016 April 2020. Website. Accessed 3 June 2020. <https://www.nparks.gov.sg/gardens-parks-and-nature/parks-and-nature-reserves>.

O'Loughlin, Eugene. *How To... Calculate Student's t Statistic (Unequal Variance) by Hand*. 9 September 2016. Video. Accessed 13 October 2020. <https://www.youtube.com/watch?v=-ukqBN5sQSI>.

Ong, Boon Lay, Andrew Ho and Kim Hin Ho. *Green Plot Ratio - Past, Present & Future*. Curtin University; National University of Singapore. Singapore, Melbourne , 2012. <https://www.researchgate.net/publication/236634754_Green_Plot_Ratio_-_Past_Present_Future>.

Parry, M.L., et al. *Assessment of adaptation practices, options, constraints and capacity. In: Climate Change 2007: Impacts, Adaptation and Vulnerability. Contribution of Working Group II to the Fourth Assessment Report of the Intergovernmental Panel on Climate Change [M.L. Parry "et al.". Eds.]*. Ed. M. L. Parry, et al. Cambridge University Press, Cambridge, UK, and New York, N.Y., U.S.A., 2007. eBook. Accessed 16 October 2020. <https://www.ipcc.ch/site/assets/uploads/2018/03/ar4_wg2_full_report.pdf>.

RevisionMaths. *Standard Deviation*. n.d. Website. Accessed 6 August 2020. <https://revisionmaths.com/gcse-maths-revision/statistics-handling-data/standard-deviation>.

Ringbell. *Relative Humidity Calculation*. n.d. Website - interactive online calculator. Accessed 1 - 25 July 2020. <http://www.ringbell.co.uk/info/humid.htm>.

Roth, Matthias and Winston T.L.Chow. "A historical review and assessment of urban heat island research in Singapore." *Singapore Journal of Tropical Geography* (2002): 17. Accessed 18 June 2020. <https://profile.nus.edu.sg/fass/geomr/roth%20chow%20sjtg12.pdf>.

Soper, Daniel. *Critical F-value Calculator*. 2020. Interactive Webpage. Accessed 13 October 2020.

Spirn, Anne Whiston. *AIR QUALITY AT STREET-LEVEL: STRATEGIES FOR URBAN DESIGN*. Boston Redevelopment Authority. Boston , 1986. PDF. Accessed 13 June 2020. <https://annewhistonspirn.com/sharefiles/Spirn-Air-Quality-1986.pdf>.

The Japan Times. *57 dead and 18,000 taken to hospitals in one week amid Japan heat wave*. Accessed 6 August 2019. Website. 28 June 2020. <https://www.japantimes.co.jp/news/2019/08/06/national/57-dead-18000-taken-hospitals-one-week-amid-japan-heat-wave/>.

URA. "URA SPACE." 2019. *ura.gov.sg.* Map. Accessed 1 October 2020. <https://www.ura.gov.sg/maps/?service=MP#>.

Urban Hub. *Taking care of urban microclimates through better design and greater energy efficiency*. 4 January 2019. Thyseenkrupp Elevator. Website. Accessed 1 July 2020. <https://www.urban-hub.com/energy_efficiency/rethinking-the-use-of-urban-microclimates/>.

Vincent, Jasmine. *Singapore CBD to see identity shift*. 28 March 2019. Website . Accessed 21 June 2020. <https://www.officescout.com.sg/news/2019/3/28/singapore-cbd-to-see-identity-shift>.

Wong, Dr Nyuk Hien. *A Study of Urban Heat Island in Singapore*. National University of Singapore. Singapore, 2002. PDF. Accessed 18 July 2020. <https://www.sde.nus.edu.sg/research/research-highlights/a-study-of-urban-heat-island-in-singapore/>.

World Bank. *Urban Population (% of total population) - Singapore*. 2018. Website . Accessed 27 June 2020. <https://data.worldbank.org/indicator/SP.URB.TOTL.IN.ZS?locations=SG&most_recent_year_desc=false>.

Xiu, Ruth Loh. *Jurong East: From swampland to Singapore's next CBD*. 21 August 2019. Website . Accessed 21 June 2020. <https://www.edgeprop.sg/property-news/jurong-east-swampland-singapore%E2%80%99s-next-cbd>.

Yajima, Arata. *THE HEAT ISLAND IN KYOTO CITY -THERMAL INERTIA OF THE URBAN AREA AND THE RURAL AREA*. Kyoto University. Kyoto, 2014. PDF. Accessed 2 July 2020. <https://www2.ges.kyoto-u.ac.jp/wp-content/uploads/2014/04/703.pdf>.

Yamato, Hiroaki, Hideo Takahashi and Takehiko Mikami. *New Urban Heat Island Monitoring System in Tokyo Metropolis*. Tokyo Metropolitan Univ., Teikyou Univ., . Yokohama: The seventh International Conference on Urban Climate, 2009. PDF. Accessed 2 July 2020. <http://www.ide.titech.ac.jp/~icuc7/extended_abstracts/pdf/375391-1-090516000046-006.pdf>.

Appendix

A

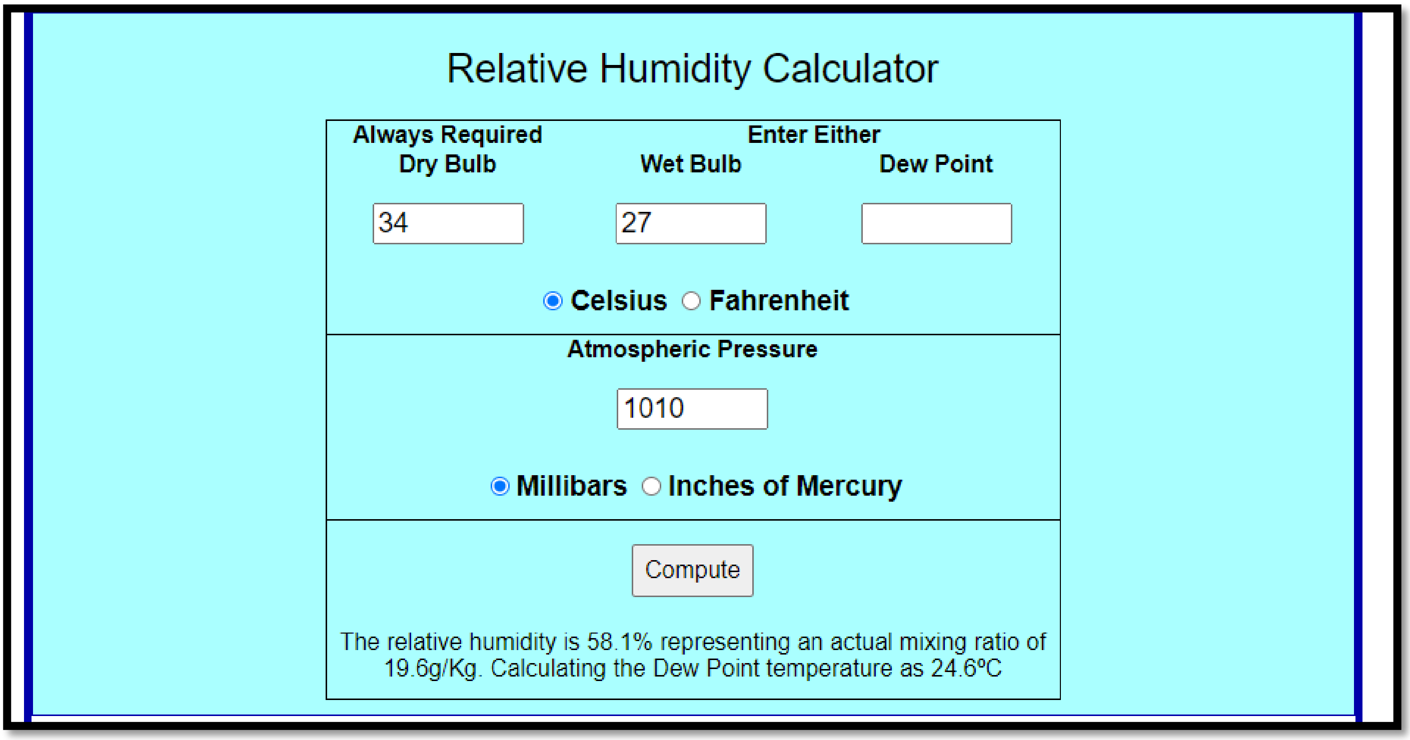

Figure 46 - RH% for site A1 at DCSG through Ringbell's online calculator

B

Data values for Light intensity that have undergone logarithmic transformation

Data point values for JE (X)

0.7853	0.2553	0.9731
0.2041	0	0.9868
1.1303	0.7924	1.4409
0.6812	0.0414	1.2504
1.0334	1.549	1.2672
0.3424	1.2122	0.8062
0.5798	0.9685	1.0128
0.4771	0.9191	1.2304
0.7076	1	0.9085
0.8573	0.6902	0.9138
0.8921	0.8808	0.9138
0.7076	0.8388	0.6812
1.1399	0.8451	1.0569
1.2041	0.7404	1.1335
1.243	0.7076	0.9243
1.179	0.6021	1.2601
0.9294	1.0334	1.5729
1.0899	0.9294	0.9191
0.7559	0.8513	0.9542
1.2279	1.2014	

Data point values for SBWR (Y)

0.2601	0.6128	0.4472
-0.1051	0.6532	1.0374
0.5798	0.6646	0.8062
1.0792	1.2014	1.5539
1.1732	1.0864	1.4116
1.5315	0.7076	1.8376
1.4579	0.8513	1.301
1.3054	0.7482	1.8069
0.6902		

$(x-\bar{x})^2$

0.0145	0.423	0.0045565
0.4921	0.8202	0.0065846
0.0505	0.0128	0.286528
0.0503	0.7469	0.1188829
0.0163	0.4139	0.1307153
0.3172	0.094	0.0098895
0.1062	0.004	0.0114942
0.1836	0.0002	0.1055099
0.0392	0.0089	8.174E-06
0.0023	0.0464	6.704E-05
0.0002	0.0006	6.704E-05
0.0392	0.0045	0.0503485
0.0549	0.0037	0.0228853
0.0891	0.0273	0.0519443
0.1138	0.0392	0.0003479
0.0747	0.0922	0.1256315
0.0006	0.0163	0.4452167
0.034	0.0006	0.000181
0.0224	0.003	0.0023636
0.1039	0.0875	

$(y-\bar{y})^2$

0.5298	0.1408	0.2925
1.1949	0.1121	0.0024
0.1666	0.1045	0.033
0.0083	0.0456	0.3203
0.0343	0.0097	0.1795
0.2954	0.0786	0.7219
0.2208	0.0187	0.098
0.1007	0.0575	0.6706
0.0887		

	X	Y
Number of data points (n)	59	25
Mean values	$\bar{x}$ = 0.9056	$\bar{y}$ = 0.988
Sum of squared differences	Σ = 6.0232	Σ = 5.5251
Degrees of Freedom	$n-1$ = 58	$n-1$ = 24
Variance	$s_x^2 = \frac{\Sigma(x-\bar{x})^2}{n-1}$ = 0.103849004	$s_y^2 = \frac{\Sigma(y-\bar{y})^2}{n-1}$ = 0.230213238

F value (larger variance divided by smaller variance)

F = s_y^2/s_x^2 = 2.216807369

Degrees of freedom 1: 24

Degrees of freedom 2: 58

Probability level: 0.05

Calculate!

Critical F-value: **1.70647557**

F(stat) = 2.2168

F(crit.)= 1.7065

F(crit.) < F(stat.)

Therefore unequal variance between groups exists

Figure 47 - Full calculation for F-statistic

C

cum. prob	$t_{.50}$	$t_{.75}$	$t_{.80}$	$t_{.85}$	$t_{.90}$	$t_{.95}$	$t_{.975}$	$t_{.99}$	$t_{.995}$	$t_{.999}$	$t_{.9995}$
one-tail	0.50	0.25	0.20	0.15	0.10	0.05	0.025	0.01	0.005	0.001	0.0005
two-tails	1.00	0.50	0.40	0.30	0.20	0.10	0.05	0.02	0.01	0.002	0.001
df											
1	0.000	1.000	1.376	1.963	3.078	6.314	12.71	31.82	63.66	318.31	636.62
2	0.000	0.816	1.061	1.386	1.886	2.920	4.303	6.965	9.925	22.327	31.599
3	0.000	0.765	0.978	1.250	1.638	2.353	3.182	4.541	5.841	10.215	12.924
4	0.000	0.741	0.941	1.190	1.533	2.132	2.776	3.747	4.604	7.173	8.610
5	0.000	0.727	0.920	1.156	1.476	2.015	2.571	3.365	4.032	5.893	6.869
6	0.000	0.718	0.906	1.134	1.440	1.943	2.447	3.143	3.707	5.208	5.959
7	0.000	0.711	0.896	1.119	1.415	1.895	2.365	2.998	3.499	4.785	5.408
8	0.000	0.706	0.889	1.108	1.397	1.860	2.306	2.896	3.355	4.501	5.041
9	0.000	0.703	0.883	1.100	1.383	1.833	2.262	2.821	3.250	4.297	4.781
10	0.000	0.700	0.879	1.093	1.372	1.812	2.228	2.764	3.169	4.144	4.587
11	0.000	0.697	0.876	1.088	1.363	1.796	2.201	2.718	3.106	4.025	4.437
12	0.000	0.695	0.873	1.083	1.356	1.782	2.179	2.681	3.055	3.930	4.318
13	0.000	0.694	0.870	1.079	1.350	1.771	2.160	2.650	3.012	3.852	4.221
14	0.000	0.692	0.868	1.076	1.345	1.761	2.145	2.624	2.977	3.787	4.140
15	0.000	0.691	0.866	1.074	1.341	1.753	2.131	2.602	2.947	3.733	4.073
16	0.000	0.690	0.865	1.071	1.337	1.746	2.120	2.583	2.921	3.686	4.015
17	0.000	0.689	0.863	1.069	1.333	1.740	2.110	2.567	2.898	3.646	3.965
18	0.000	0.688	0.862	1.067	1.330	1.734	2.101	2.552	2.878	3.610	3.922
19	0.000	0.688	0.861	1.066	1.328	1.729	2.093	2.539	2.861	3.579	3.883
20	0.000	0.687	0.860	1.064	1.325	1.725	2.086	2.528	2.845	3.552	3.850
21	0.000	0.686	0.859	1.063	1.323	1.721	2.080	2.518	2.831	3.527	3.819
22	0.000	0.686	0.858	1.061	1.321	1.717	2.074	2.508	2.819	3.505	3.792
23	0.000	0.685	0.858	1.060	1.319	1.714	2.069	2.500	2.807	3.485	3.768
24	0.000	0.685	0.857	1.059	1.318	1.711	2.064	2.492	2.797	3.467	3.745
25	0.000	0.684	0.856	1.058	1.316	1.708	2.060	2.485	2.787	3.450	3.725
26	0.000	0.684	0.856	1.058	1.315	1.706	2.056	2.479	2.779	3.435	3.707
27	0.000	0.684	0.855	1.057	1.314	1.703	2.052	2.473	2.771	3.421	3.690
28	0.000	0.683	0.855	1.056	1.313	1.701	2.048	2.467	2.763	3.408	3.674
29	0.000	0.683	0.854	1.055	1.311	1.699	2.045	2.462	2.756	3.396	3.659
30	[illegible]	[illegible]	[illegible]	[illegible]	[illegible]	[illegible]	2.042	2.457	2.750	3.385	3.646
40	0.000	0.681	0.851	1.050	1.303	1.684	2.021	2.423	2.704	3.307	3.551
60	0.000	0.679	0.848	1.045	1.296	1.671	2.000	2.390	2.660	3.232	3.460
80	0.000	0.678	0.846	1.043	1.292	1.664	1.990	2.374	2.639	3.195	3.416
100	0.000	0.677	0.845	1.042	1.290	1.660	1.984	2.364	2.626	3.174	3.390
1000	0.000	0.675	0.842	1.037	1.282	1.646	1.962	2.330	2.581	3.098	3.300
z	0.000	0.674	0.842	1.036	1.282	1.645	1.960	2.326	2.576	3.090	3.291
	0%	50%	60%	70%	80%	90%	95%	98%	99%	99.8%	99.9%
	Confidence Level										

Figure 48 - t-table to find critical value (Gerstman)